A FREQUENCY-BASED CONTEXTUAL CLASSIFICATION APPROACH TO THEMATIC LAND COVER MAPPING USING PANCHROMATIC SATELLITE IMAGE DATA

THESIS

Presented to the Graduate Council of
Southwest Texas State University
in Partial Fulfillment of
the Requirements

For the Degree

Master of Applied Geography

By

Matthew E. Ramspott

San Marcos, Texas
May, 2000

This work is dedicated to the memory of
my grandfather, Arthur Ramspott,
whose generosity, inventiveness, hard work, and character
were of great inspiration to me.

ACKNOWLEDGEMENTS

This work would not have been possible but for the instruction, mentoring, and advisement of my thesis supervisor, Dr. Ron Eyton. His enthusiasm and technical wizardry place him among the most effective teachers I have known. I owe much gratitude as well to Dr. Fitzsimons and Dr. Showalter of the Southwest Texas State University Geography Department for the development of this manuscript. Thanks also go to Dr. Rich Dixon for help with climatological data. Thanks go to Teresa Howard and Dr. Gordon Wells of TNRIS for assistance with locating the Landsat-7 data used for this research. I also owe a debt of thanks to Dr. Jon Kimerling of Oregon State University and to Dr. David Wishart of the University of Nebraska for sparking my interest in cartography and geography in the first place.

A list of thanks would not be complete without a few personal acknowledgements. Thanks go to my mother and father for supporting my unique interests even though they haven't always understood "just what it is I'm doing". Thanks go to many friends in Lincoln, Corvallis, and San Marcos for their ideas and support over the years. Finally, I would like to extend special gratitude to Rebecca Bycott. Without her boundless patience, love, and positive energy, this work would surely not have been possible.

This thesis was submitted to the committee on April 10, 2000.

TABLE OF CONTENTS

LIST OF TABLES

LIST OF FIGURES

CHAPTER I

INTRODUCTION

The expansion of cities and suburbs throughout the industrialized nations of the world is an often studied and much documented phenomenon in geographic research. Central Texas is an area that particularly lends itself to study in this regard, as it has recently experienced dramatic and rapid changes due to urbanization. Urban sprawl, expedited by land speculation, leads inevitably to the loss of rural land that has high potential for other uses. The expansion of sprawl results in the subjugation of open land for many purposes, including residential housing developments, urban and commercial services, infrastructure development, and land uses related to resource extraction or other industrial processes.

These changes are of considerable concern to planners for a variety of reasons, underscoring the importance of having an available (and relatively inexpensive) means of tracking these developments in order to assess their social and environmental impacts. Tracking changing land use patterns is important when trying to predict and plan for future impacts on natural areas and the diminishing supply of lands available for agricultural production. The overall effectiveness and feasibility of planning for water availability, transportation infrastructure, and community base development (e.g., schools, hospitals, police and fire protection) is impacted by the onset of rapid urban development and by the redevelopment of intra-urban areas into different land uses. Remote sensing can provide a partial solution to the complex problems associated with the reliable and frequent updating of spatial planning information.

Remote sensing has proven to be a useful tool for monitoring the nature and dynamics of urban sprawl (Charbonneau et al. 1993), particularly when used in conjunction with census statistics and other geographic data. Satellite remote sensing is often used as a method for updating information that has been derived from the more detailed data provided by aerial photography surveys. The primary drawback of aerial survey as used in land cover mapping is that the data cannot be frequently updated due to prohibitive cost. This problem can be addressed quite readily using satellite remote sensing data in conjunction with the powerful and highly flexible tools made available by modern information technology and geographic information systems (GISs). The use of remotely sensed data has played an increasingly greater role in geographic planning and in environmental monitoring and management projects around the world. However, remote sensing studies themselves are not without limitations. Barring extensive and expensive expert human interaction and interpretation, remote sensing is capable of giving information only about the physical properties of the land surface that is being imaged. The land use and land cover characteristics of landscapes that are undergoing urbanization are highly anthropogenic in nature. Realizing the full potential of remotely sensed data necessitates a determination of the relationship between the physical land surface information given by satellite data and the corresponding functional properties of the elements found on this surface. This problem generally presents a major limitation to the thematic mapping applications of remote sensing (Charbonneau et al. 1993). The research outlined in this paper is generally directed toward the exploration of this problem through the use of techniques which can enhance the traditional capabilities of an automated image classification algorithm, thereby improving the usefulness of the mapping units making up the classified image map. It should be emphasized that this process can never be fully automated, and must remain an interactive and partially subjective one. Knowledge of human and physical geography is of penultimate importance when processing remotely sensed data into map products that are useful for both planning and for scientific monitoring and modeling. The underlying purpose of this research is to find ways to expedite, enhance, and simplify this process for the image interpreter, scientist, and geographer.

CHAPTER II

BACKGROUND AND RESEARCH OBJECTIVE

Pattern Recognition

Automated pattern recognition is a quantitative, adaptable, computer executed methodology that is ideal for applications in remote sensing (Swain and Davis 1978). Allowing for repeatable processing of large parcels of image data through computerized algorithms, pattern recognition provides a way to quickly generate dasymetric maps that reduce the vast amount of data present in imagery into a generalized form that is more immediately accessible to the resource manager or planner. Pattern recognition is typically applied to digital data in the form of a multispectral classification based on the per-pixel spectral responses in each image band. In general, the classification technique involves dividing the data space (sometimes called multispectral space or measurement space) into decision regions, each corresponding to a discriminable class. Various logic systems can be employed in the implementation of multiband image classification, and are described in adequate detail in the literature (Swain and Davis 1978; Richards 1993; Lillesand and Kiefer 1994; Jensen 1996). The applications of pattern recognition using digital image data are widespread, ranging from thematic maps of land cover derived from single date satellite images (Fuller 1994) to pattern change detection maps (Jensen 1981), and even to the classification of land cover by digitally processing aerial photography (Tsu 1978; Scarpace and Quirk 1980). Much research has attempted to automate the process of mapping land cover and land use of urban and urban fringe areas using classification of satellite data (Jensen 1979; Forster 1980; Jackson et al. 1980; Jensen and Toll 1982; Toll 1984; Moller-Jensen 1990).

Problems with Conventional Classification Methods

Conventional per-pixel classification is dependent upon the assumption that useful classes can be differentiated on the basis of spectral information alone. This assumption is frequently not met, leading to unacceptable levels of classification error, or to the development of classes that are not spatially cohesive enough to be of any use. The nature of a visible/near visible wavelength remote sensing system is that it records the radiant flux from a mixture of biophysical materials within the instantaneous field of view (IFOV) of the sensor (Jensen 1996). The IFOV is for practical considerations the same as the pixel resolution of the product data. A pixel generalizes this mixture of spectral responses into one representative value. Thus a pixel is almost always "mixed," except in the case of the imaging of geographic features which are homogeneous at scales similar to the pixel resolution. This mixed pixel problem is particularly prevalent in imagery covering areas that are markedly heterogeneous at large map scales, such as that covering high density urban and suburban landscapes, industrial areas, transportation networks, and communications and utilities infrastructure. Conventional image classification methods in general have been relatively unsuccessful in discriminating land use within these areas.

This mixed pixel problem has been described as one of "scene noise," especially in scene portions which are characterized by a high degree of heterogeneity (Barnsley and Barr 1996). This type of noise is manifest in the “salt and pepper” effect that is typically evident in conventional classifications of such scene portions. In areas where individual ground cover elements within a pixel begin to dominate pixel response, the overall spectral return from the pixels in the area becomes more varied, leading to difficulties with meaningful scene classification. One simple technique that might be used to counter this effect is the application of a median filter to the classified image map, which can help to remove the salt and pepper.

Wharton (1982b) points out a compounding problem which surfaces with imagery of high spatial resolution. "Land use" classes are necessarily not the same as the "land cover" classes separated out of imagery by conventional classification techniques. Land use classes, defined by some degree of homogeneity in terms of cultural or geographical considerations, may be "resolved into two or more spectrally dissimilar [ground cover] components" (Wharton 1982b, p. 317). In some cases, the same ground cover type may constitute different land uses based on the location and context in which it is found. Furthermore, when using remotely sensed imagery to make land use maps of cities and towns, even high-resolution imagery suffers from the aforementioned noise effects (Barnsley 1996). This differentiation between the concepts of cultural land use and physical land cover is further discussed in other studies (Forster 1980; Gong and Howarth 1992; Eyton 1993; Sharma and Sarkar 1998).

The persistent problems associated with classifying urban and suburban land use have been a predominant theme in remote sensing research for some time, yielding numerous approaches for defining and addressing the shortcomings of conventional per-pixel classification. One might hazard the question; why try to use digital data at all in attempting to produce useful maps of land use and land cover in urban and urban fringe areas? Jensen (1979, p. 400) suggests the practical response that "manual interpretation of large-scale aerial photography, although accurate, is becoming increasingly expensive, whereas machine-assisted analysis of small scale imagery is relatively inexpensive and has the potential of being just as accurate," especially with the inclusion of certain modifications to the conventional techniques. A good overview of the literature covering the various methods that have been devised as modifications or enhancements to per-pixel classification is given in Barnsley and Barr (1996). Two recurring concepts in these research efforts are the use of image texture (Haralick and Sharmugan 1974; Hsu 1978; Jensen 1979; Gong and Howarth 1990) and the use of pixel context information (Wharton 1982a; 1982b; Gong and Howarth 1992; Eyton 1993; Barnsley and Barr 1996; Sharma and Sarkar 1998; Howard 1998) in the improvement of the classification procedures.

Early research focuses on the per-pixel extraction of various measures of image texture, such as measures of contrast, high frequency information, second angular moment, or entropy, for use in automated classification systems (Haralick and Sharmugan 1974; Hsu 1978; Jensen 1979). These measures are typically incorporated into a classification system along with the spectral information, yielding some improvement in automated classification of urban-fringe areas. Jensen (1979) cautions that this improvement is small in proportion to the expense of additional data processing. In somewhat similar fashion, Gong and Howarth (1990) analyze the effect of incorporating edge density information as an additional band of data into a conventional multispectral classification system, also leading to an improvement of overall classification accuracy.

Frequency-Based Contextual Classification

Wharton (1982a; 1982b) proposes a different type of classification processing — one which uses a measure of pixel context. The method employed is a two stage process which first separates the image cover types with a normal per-pixel analysis, assuming that the cover types are spectrally separable. The method then reclassifies the pixels based on a per-pixel vector of cover type frequencies, generated by roving a square kernel through the classified image pixel by pixel. This technique, referred to as "CONAN" or "context analysis" by Wharton, has also been applied with some variations in other research (Gong and Howarth 1992; Eyton 1993; Howard 1998), affording it the more specific label *frequency-based contextual classification* (FBCC). Overall this technique is appropriate to addressing the issue of determining the *land use* class associated with a particular assemblage of constituent *land cover* types, in that it classes a pixel based on the frequency of occurrence of various cover types within the vicinity of that pixel. The dimensions of the kernel determine the number of pixels considered as the unit of analysis for assessment of context, and hence the level of generalization present in the final map. The FBCC applied to medium and high-resolution urban image data by Eyton (1993) and by Howard (1998) is quite similar to the technique that is to be explored in this paper. This particular method could be described as aspatial, in that the reclassification of image pixels is made solely on the basis of the frequency of occurrence of the various cover type classes that are derived in the first stage of the process.

The advanced contextual analysis technique employed by Barnseley and Barr (1996) does make use of the spatial arrangement of pixel classes in addition to the frequency of classes present within a roving kernel. This rigorous treatment, which is accomplished through the development of "adjacency-event matrices," may be limited by computational intensity at kernel sizes much larger than 3x3 or 5x5 pixels. It has been suggested that a kernel size of less than 15x15 pixels may not be appropriate for frequency-based contextual classifications, at least when dealing with medium to high-resolution data (Eyton 1993).

In summary, the use of FBCC has been shown to provide a valid and useful approach to the enhancement of conventional procedures for classification of land cover with scenes where conventional per-pixel classification is relatively ineffective. The technique of frequency-based contextual classification, along with other techniques attempting to utilize pixel context and spatial texture in a digital image, has proven useful for the extraction of thematic information, particularly when dealing with desired mapping units that are made up of pixel assemblies with relatively heterogeneous spectral properties.

Application of FBCC to Single-Band Imagery

In many applied contexts, multispectral imagery may not be readily available, forcing the analyst to make use of single-band digital imagery or panchromatic aerial photographs. Minimizing costs and maximizing the usefulness of available imagery is often of considerable priority in application. For some projects, such as those involving the use of historical data in the form of aerial photographs, multiband imagery is simply not an option. The use of single-band imagery precludes the automated extraction of thematic information by conventional means of multispectral classification. However, the incorporation of pixel context information into a modified classification algorithm such as FBCC may prove to be a useful procedure for generating land use and land cover maps using panchromatic imagery. A search of the literature yielded very few examples of automated classification derived from single-band imagery. One notable study employed a "texture feature extractor" in the form of a roving kernel which extracted various measures of image texture, used with some success in classifying land cover from digitized panchromatic high altitude aerial photography (Hsu 1978, p. 1393).

Research Objective

The objective of this research is to show that the concept of frequency-based contextual classification can be applied, with some modification, to generate useful land use/land cover classification maps from single-band, panchromatic digital imagery.

CHAPTER III

IMAGE DATA AND STUDY AREA

Landsat-7 ETM + Image Data

Image data from the Landsat-7 Enhanced Thematic Mapper Plus (ETM+) sensing system were used as a source material for the automated classifications presented in this paper. This imagery was chosen in order to allow a comparison of the classified image map produced using a panchromatic image with that produced by a more conventional multispectral analysis. The ETM+ system consists of 6 bands of visible/near visible reflectance data at 30-meter resolution and one panchromatic band at 15-meter resolution, all acquired simultaneously and distributed in a georegistered format (the image data set also contains two channels recording emitted thermal radiation, which were not considered as part of this study). The fact that the ETM+ imagery used here consisted of both a six dimensional multispectral data set and a one-dimensional panchromatic data set allowed both types of FBCC analysis to be performed. Additionally, the simultaneous acquisition of the panchromatic and multispectral data allowed the production of classified image maps registered to the same map projection and coordinate system. As a further benefit, these maps could be compared to each other with certainty that any differences were not due to temporal changes. Landsat Thematic Mapper (TM) data generated from Landsat-4 and Landsat-5, which is essentially comparable to the set of multispectral bands in the ETM+ data, has been used commonly in research and applications involving the thematic mapping of land use in urban and suburban areas (Toll 1984; Moller-Jensen 1990; Fuller 1994).

A nearly cloud free ETM+ scene covering the vicinity of Austin, Texas was acquired by Landsat-7 on September 18, 1999 and telemetered by a downlink to a NASA receiving station on the ground. Georegistration, terrain correction, radiometric calibration, and other processing were done at the United States Geological Survey (USGS) Earth Resources Observation System Data center in Sioux Falls, South Dakota. This data set was subsequently made available for use in this research by the Texas Natural Resources Information System (1999) in Austin. Table 1 lists the map projection parameters and general acquisition information that were associated with this imagery and also lists the image bandwidths, or the portion of the electromagnetic spectrum that was recorded by each image band. The panchromatic channel of the ETM+ imagery, which is of primary interest in this study, recorded a range of radiation from 0.5 μm to 0.9 μm, corresponding roughly to a range that extends from visible green radiation into the near-infrared part of the spectrum. This characteristic of the panchromatic channel was ultimately quite important to the interpretation of classification results.

The ETM+ scene used for this research contained a variety of land cover types, ranging from undeveloped, forested hills and bluffs to rolling prairies devoted to production agriculture, and from high density urban and built up land to industrial tracts, major transportation networks, and low density suburban sprawl. Figure 1 shows, in the form of a "footprint" map, the extent of the imagery considered in this study. The footprint of the entire ETM+ scene is outlined in bold yellow. This area consisted of

Table 1. Landsat-7 ETM+ Imagery Characteristics

PROJECTION PARAMETERS		
Projection: UTM Zone 14 N		
Earth Ellipsoid: WGS 84		
ACQUISITION DATA		
WRS Path 27, Row 39		
Acquisition Time: September 18, 1999, 16:55 Z		
Sun Elevation: 55.43°		
Sun Azimuth: 139.67°		
ETM+ CHANNEL BANDWIDTHS		
Band	Color	Wavelength Range (μm)
1	Blue	0.45 – 0.52
2	Green	0.52 – 0.60
3	Red	0.63 – 0.69
4	Near IR	0.76 – 0.90
5	Mid IR-1	1.55 – 1.75
7	Mid IR-2	2.08 – 2.35
8	Panchromatic	0.5 – 0.9

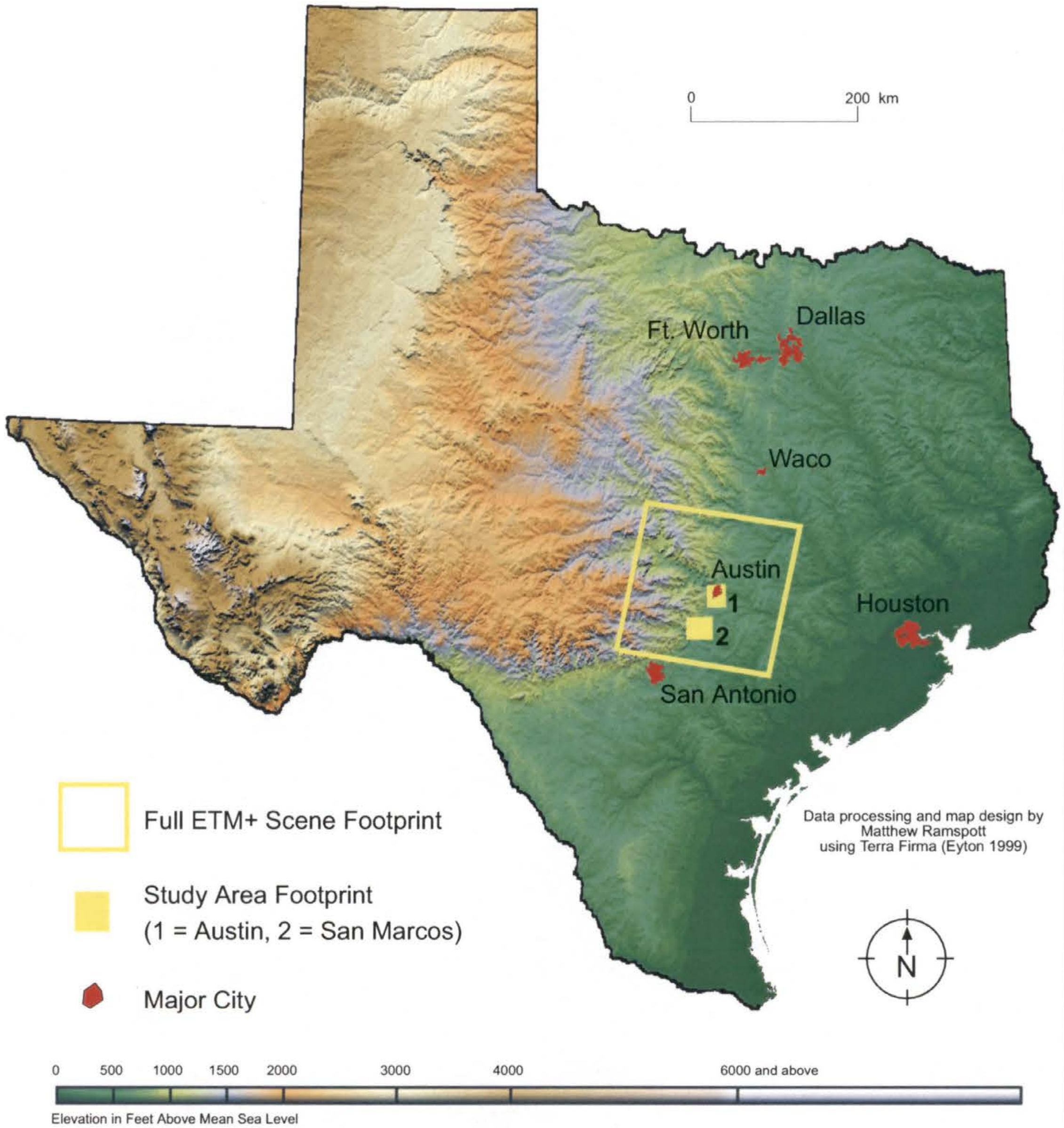

Figure 1. Physiographic map of Texas showing the study location.

approximately 34,300 square kilometers of ground coverage (about 13,255 square miles). In the panchromatic band (15 meter resolution) the scene consisted of a raster grid of 13,926 rows and 14,818 columns, for a total of 206,355,468 pixels of information. This information is summarized in Table 2, along with the geographic coordinates bounding the scene, and with the corresponding information for the six multispectral bands.

ETM+ imagery has a color depth of 8 bits (1 byte) per band. An 8-bit image is one that potentially contains 256 gray level values (GLVs). In the data acquired from most modern civilian remote sensing platforms, the full range of 256 values is seldom fully utilized. This is largely due to limitations in the radiometric sensitivity of the sensor. The ETM+ panchromatic channel does use the full range of gray level values, although the majority of the data still fall within a relatively narrow range (this will be discussed in greater detail below). In the full ETM+ scene, the image bands were padded with zero values in the areas where the de-skewing of the imagery left blank spaces in the rectangular data storage grid.

Due to practical data storage limitations, and in the interest of imposing limits on computer processing time, the processing of the entire ETM+ scene in a single classification operation was not deemed feasible. Subsetting was performed on the ETM+ data to select areas of analysis of more manageable size. By taking care to select subsets from the interior of the scene, this procedure was done in such a way as to eliminate the problem of dealing with the absence of data in the edge portions of the image. Given adequate data storage space and computer processing power, the classification of an entire ETM+ scene by the methodology presented in this paper would theoretically be possible.

Table 2. Scene Footprint and Data Set Size Information

FULL SCENE		
BOUNDING COORDINATES		
Upper Left: 31°13'49" N, 98°36'18" W	Upper Right: 30°57'25" N, 96°42'55" W	
Lower Left: 29°38'41" N, 99°00'17" W	Lower Right: 29°22'35" N, 97°08'42" W	
FOOTPRINT		
Footprint Dimensions: 185 km x 185 km		
Land Area Covered: 13,255 sq. miles (34,330 sq. km)		
PANCHROMATIC		
Pixel Rows: 13926	Pixel Columns: 14818	Data Set Size: 206.36 MB
MULTISPECTRAL (6 BANDS)		
Pixel Rows: 6963	Pixel Columns: 7409	Data Set Size: 51.59 MB per band
SUBSET 1: AUSTIN		
BOUNDING COORDINATES		
Upper Left: 30°21'33" N, 97°51'36" W	Upper Right: 30°21'25" N, 97°38'13" W	
Lower Left: 30°07'45" N, 97°51'45" W	Lower Right: 30°07'38" N, 97°38'24" W	
FOOTPRINT		
Footprint Dimensions: 25.500 km x 21.450 km		
Land Area Covered: 547 sq. km		
PANCHROMATIC		
Pixel Rows: 1700	Pixel Columns: 1430	Data Set Size: 2.43 MB
MULTISPECTRAL (6 BANDS)		
Pixel Rows: 851	Pixel Columns: 716	Data Set Size: 0.61 MB
SUBSET 2: SAN MARCOS		
BOUNDING COORDINATES		
Upper Left: 30°00'58" N, 98°07'26" W	Upper Right: 30°00'49" N, 97°48'18" W	
Lower Left: 29°47'10" N, 98°07'33" W	Lower Right: 29°47'02" N, 97°48'28" W	
FOOTPRINT		
Footprint Dimensions: 25.500 km x 30.750 km		
Land Area Covered: 784 sq. km		
PANCHROMATIC		
Pixel Rows: 1700	Pixel Columns: 2050	Data Set Size: 3.48 MB
MULTISPECTRAL (6 BANDS)		
Pixel Rows: 850	Pixel Columns: 1025	Data Set Size: 0.87 MB per band

Study Area

Two imagery subsets were chosen. The bounding geographic coordinates and data set sizes of these subsets are given in Table 2. Subset 1 was centered on central Austin, Texas (Travis County) and consisted primarily of inner urban and suburban residential areas, major highway transportation corridors, major commercial and business districts, airports, and, to a lesser extent, some areas of exurban land. Subset 2 was centered roughly on San Marcos, Texas and was situated in such a way as to include the communities of Wimberley and Kyle, significant areas of newly developing exurban land in both Hays and Caldwell Counties, natural woodlands, rangelands, agricultural land, and riparian areas. The spatial extent of these two subsets in relation to the full ETM+ scene extent is depicted in Figure 1. This map also depicts the dramatic change in elevation associated with the Balcones Escarpment (visible as the line of rapid change from green to yellow to gray in the elevation scheme, stretching from Austin to west of San Antonio). The city of Austin, Texas is located where the Colorado River crosses this escarpment. San Marcos, Texas is situated along the Interstate 35 corridor approximately 30 miles to the southwest of central Austin, at the spring-fed headwaters of the San Marcos River. Both image subsets are bisected by the edge of the escarpment and contain significant portions of both the Hill Country to the west and the Blackland Prairies to the east of this important physiographic division.

The Texas Hill Country lies on the eastern edge of the greater Edwards Plateau physiographic region. The natural land surface of the Hill Country consists almost entirely of a thin, limestone-based soil which is covered with a medium to thick growth of juniper, live-oak, and mesquite, and with a varying growth of prickly pear and other cacti (Ramos 1997). Within the study area, this region is characterized by range areas cleared of trees and by ranches and residential subdivisions in addition to the natural juniper/live-oak woodlands. Some residential areas, currently under construction, consist only of roads and ground disturbances. The Blackland Prairies are characterized by a much darker, richer soil that is used extensively for agriculture. This area is dotted with numerous small ponds and reservoirs, and shows the familiar rectangular patterns of land that has been subjected to regular cultivation.

Climate

The climate of the study area is categorized as humid subtropical with hot summers and mild winters (Wood 1996). The Köppen climate classification is Cfa (Strahler 1978). Precipitation is usually distributed fairly evenly throughout the year, with the heaviest amounts of rainfall normally occurring during late spring. There is a secondary normal precipitation peak occurring in September, which is primarily due to tropical cyclones moving inland from the Gulf of Mexico during this season. Precipitation during the summer months is generally associated with thunderstorms. Often large amounts of rain will fall within a short period of time. Precipitation during the winter months generally consists of light rain. Snowfall in the area is typically negligible. For Austin, the warm season, as measured by the freeze-free period of a year, has an average length of 273 days (Wood 1996). Figure 2 shows the monthly 30-year normal precipitation levels (1960-1990) and average temperatures for two weather stations representative of the Austin (Figure 2a) and San Marcos (Figure 2b) areas.

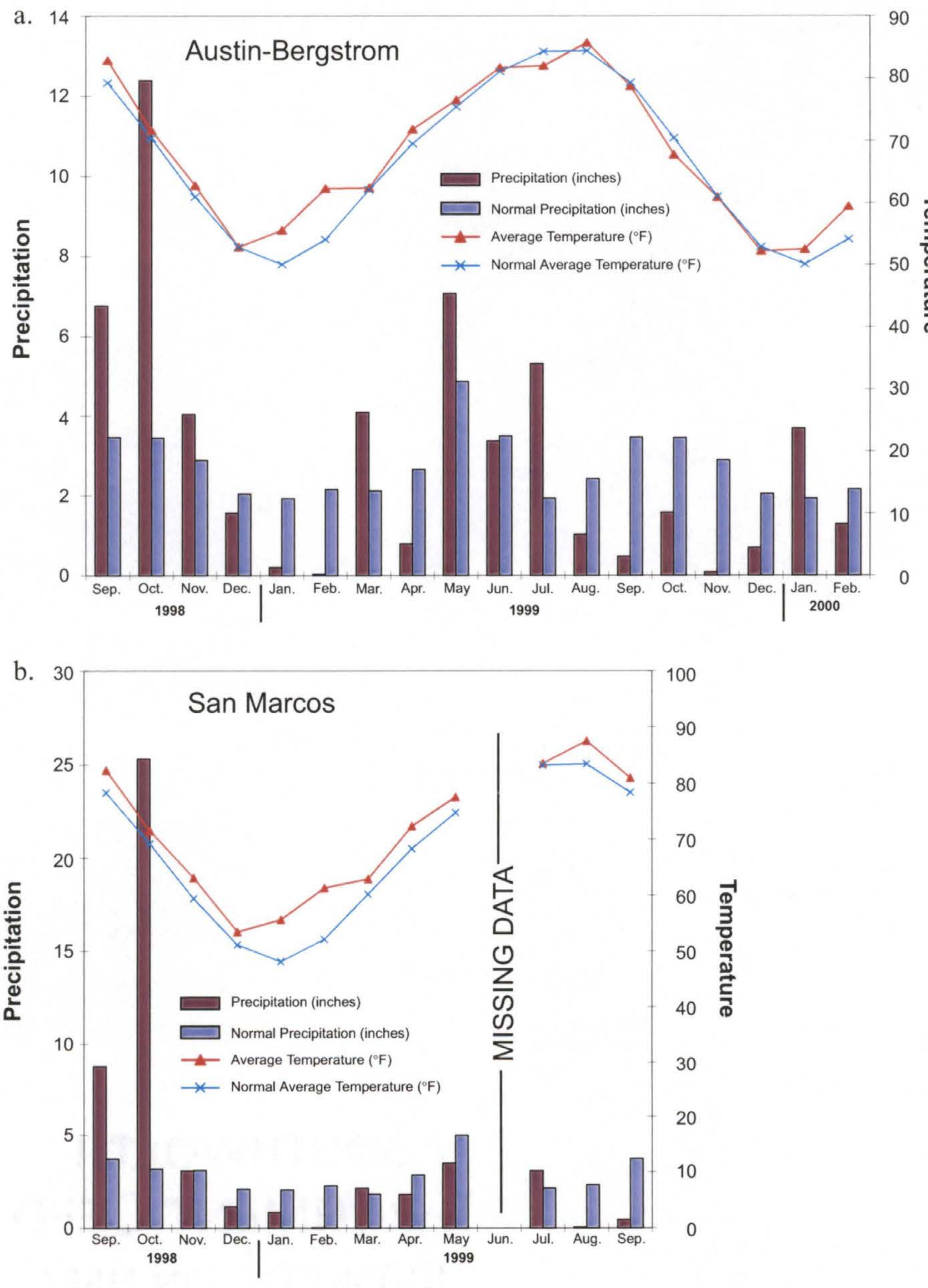

Figure 2. Climate data for the Austin-Bergstrom (a) and San Marcos (b) weather stations.

Figure 2 also shows the monthly precipitation and temperature data for the year preceding the acquisition of imagery in September 1999. The rainfall peak in October 1998, which is especially marked for the San Marcos weather station, is associated with a notable record rain and flood event which occurred on October 17-20, affecting large areas of Central Texas including the communities of Austin, San Marcos, New Braunfels, San Antonio, Seguin, and Victoria, and the lower San Antonio, Guadalupe and Colorado River Basins. Other than this significant event, which occurred almost a year before image acquisition, the climatographs also indicate a drier and warmer than normal winter for 1998/1999 and a slightly drier than normal period for the two months preceding imagery acquisition. Such marked departures from normal levels of precipitation and temperature are quite typical of the climate of Central Texas, and in this case were not deemed to be problematic in terms of an effective interpretation of classification results. The dry months of July and August 1999 are likely to have had an effect on the signatures found in the ETM+ imagery acquired in September, and this was taken into account as much as possible upon analyzing the land-cover information. The climatograph for the Austin-Bergstrom Airport weather station (Figure 2a) has been extended to include the months through February of 2000 to allow an assessment of the effect of climatic variation on the character of the ground-based photography collected during field survey.

CHAPTER IV

METHODOLOGY

The following steps were used to investigate the use of panchromatic satellite imagery for frequency-based contextual classification of land use/land cover.

1. Suitable imagery was selected as source material for a classification, and data subsets were chosen.
2. Important geographic details of the study area were researched and outlined, including climatography, physiography, and human geography and land use.
3. A suitable set of data processing steps was developed for the application of the FBCC to the data.
4. The appropriate level of generalization (kernel size) and steps for post-processing were considered in order to maximize the usefulness of the classified image maps that were produced. A systematic procedure for development of a map legend was created based upon human interpretation of the imagery during various levels of classification processing and upon other sources of information about the subject area, including ground truth.

5. A method was devised for comparison of the results of the non-conventional, panchromatic classification with classifications derived using a more traditional multispectral processing algorithm.

Items 1 and 2 were covered in detail in the previous chapter. The details of items 3, 4 and 5 are presented in this section.

Outline of Data Processing Procedures

This section offers a technical overview of the techniques used to perform classifications of the ETM+ data, and of the GIS and image processing software and techniques employed in the classification analysis and data visualization. One topic to be discussed is the specific technique of per-pixel analysis that was utilized, including the procedures used both for the statistical clustering of an unsupervised training sample, and for the discrimination of classes in the imagery based upon the training clusters. This common per-pixel classification was utilized in the FBCC process whether dealing with multiband or single-band data, as will be shown. The relevant details of the FBCC procedure as it has traditionally been applied to multispectral data, and as it was applied here for purposes of comparison with the single-band classification results, will be outlined. The specific modifications to the FBCC technique necessary for its application to a single band of image data will be described. Most of the data processing for this research was performed using Terra Firma, a set of DOS-based image processing and data analysis software modules created by Eyton (1999). This software contains specific programs for implementing FBCC. The procedures employed in the development of a legend for a classification map, in the comparative analysis of the panchromatic and multispectral classification systems, and in the post processing of the classification maps will then be discussed.

Per-Pixel Classification

The first step in a multidimensional per-pixel classification is to obtain a representative sample of the population of pixels in an image for use in the training of the automated classifier. Two approaches commonly used to accomplish this are supervised and unsupervised training sample selection. In the supervised approach, the analyst picks the training sample based on preliminary image interpretation; in the unsupervised approach, the training data are collected by a systematic random sample (Lillesand and Kiefer 1994). Due to the exploratory nature of this project, the unsupervised training sample selection method was deemed more appropriate than the supervised method. Performing a classification with a minimum of a priori user intervention seemed to be the best course of action in attempting to gauge the strengths or weaknesses of an untried method. In this case, the training sample was collected by designating that every i_{th} pixel from every j_{th} row of the scene to be classified would be selected. This training sample was then processed using the TRAIN module of Terra Firma (Eyton 1999), a k-means cluster analysis algorithm that finds natural groups of pixels in multidimensional data space. This technique, which allows the analyst to select the number of desired clusters at the outset, begins by arbitrarily "seeding" that number of cluster centers in data space. Each pixel, represented as a point in data space, is then assigned to the cluster whose centroid is the closest. The process then repeats itself, after recalculating the locations of the centroids, continuing iteratively until the cluster centroids stabilize to a satisfactory degree (Lillesand and Kiefer 1994).

One advantage of the k-means clustering technique as it is applied in the TRAIN module of Terra Firma (Eyton 1999) is that it allows the user to calculate an overall F-ratio (between-group variance divided by within-group variance) for a range of numbers of classes. This affords the user some knowledge about the optimum number of natural groups to be found in the data. In each classification that was undertaken, the number of clusters into which to group the training sample data was determined by examining the F-ratio for all numbers of natural groups between 5 and 15 (the target range for the number of classes in the final map), and then selecting a local maximum of the F-ratio. By maximizing the variance between groups at the same time as minimizing the variance within each group, certainty was increased regarding the true separability of the groups. In all cases the lowest (or the only) optimum number of classes between 5 and 15 was chosen.

The second step in the per-pixel multidimensional classification procedure is the classification stage, in which the training field data are used to make a division of the data space, which then is used to classify the entire data set. There are numerous approaches for accomplishing this task (Swain and Davis 1979; Richards 1993; Lillesand and Kiefer 1994; Jensen 1996). The per-pixel technique used in this paper was the CLASS module of Terra Firma (Eyton 1999), which applies a common classification logic system that is relatively simple to implement (Eyton 1993). The algorithm used is based on the discriminant analysis classification functions developed by Fisher (1936).

This technique is a forced classifier, meaning that every pixel in the subject image will be assigned to a class, leaving no unclassified pixels.

Frequency-Based Contextual Classification

Figure 3 illustrates the processing algorithm utilized in FBCC as it was applied with Terra Firma (Eyton 1999). This process, when traditionally applied to multispectral data, consists of two separate applications of the conventional per-pixel classification. The critical step unique to FBCC is the series of convolutions producing the maps showing per-pixel frequency counts for each cover type. These maps are then treated as "bands" of multidimensional data and are reprocessed using essentially the same per-pixel technique as before. The result is a map that is somewhat more generalized than the one generated by a simple per-pixel classification. The level of generalization depends in large part on the size of the kernel used to extract the context information. For this study, preliminary research was conducted to find the optimal kernel size for the 15-meter resolution of the data used in this particular case; kernel sizes of 7x7, 15x15, and 31x31 pixels were used.

FBCC With Panchromatic Imagery

Only the initial step of the FBCC processing algorithm needed changing to modify the procedure for use with a single band of data. The panchromatic image had to be "classed" using a one-dimensional image classification scheme in this initial stage. The technique of level slicing, which is typically used to highlight and show detail in image areas of similar gray level, can be thought of in a different way when it is used to

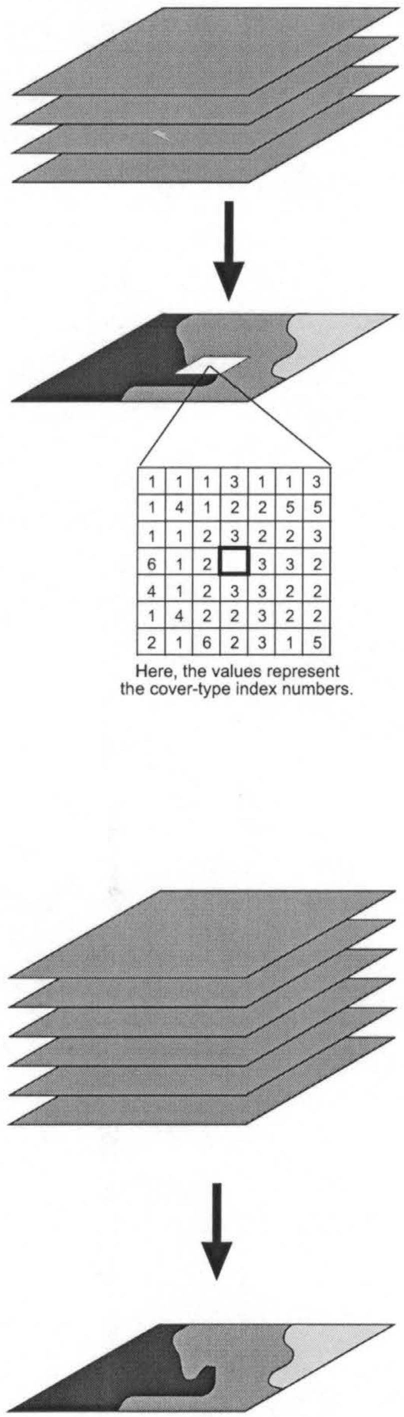

Multiband imagery are processed using conventional per-pixel classification techniques.

For a panchromatic image, this step consists of a simple one-dimensional classification of the brightness values.

The result is a digital map divided into N land cover types based only on spectral responses.

A square kernel roves through the map of cover type classes counting the frequency of occurrence of a class within the neighborhood associated with each image pixel, as defined by the kernel size. This convolution is repeated N times, once for each class.

Each iteration produces a separate map showing the frequency of occurrence for a single class, producing a total number of maps equal to N, the number of classes discriminated in the initial step.

These N maps are then processed as an N-dimensional per-pixel classification in which cover type frequencies are classified, rather than brightness values. The result is a single dasymetric digital map showing the contextually reclassified cover-type assemblies.

Figure 3. Frequency-based contextual classification, using Eyton's (1993) method.

map or class ranges of brightness into particular shades of gray. According to Richards (1993, p. 107), "When used generally to segment a scalar image into significant regions of interest, [level slicing] is acting as a simple one-dimensional parallelpiped classifier." A review of the various methods of single variable cartographic representation provided several potential options for accomplishing level slicing (Slocum 1999), including equal-frequency, equal-interval, and other common methods of single variable classification.

First Stage of Panchromatic Classification: Level Slicing

Figure 4 illustrates the procedure that was utilized to achieve the first stage of classification for the panchromatic data in this study. The histogram of the sample image subset given in Figure 4a was unimodal. This is typically the case for satellite imagery which does not cover a large area of both very light pixels such as sand or ice and very dark pixels such as deep water. Both of the panchromatic image subsets that were classified in this study showed similar, unimodal histogram characteristics. For the sample subset illustrated in Figure 4, the majority of the data distribution falls between the gray level values of 45 and 82. This type of distribution, with most of the data contained within a relatively narrow range, is typical of this ETM+ scene as a whole, and of most commercially available satellite imagery in general.

Figure 4b shows a detailed portion of the histogram found in Figure 4a, and depicts the class divisions necessary to divide the data into 10 equal-frequency classes. Class limits were chosen simply by examining a table showing accumulated frequency as the data ranged from Gray Level 0 to Gray Level 255. The equal-frequency technique was chosen primarily for its ease of computation and simplicity of implementation. An

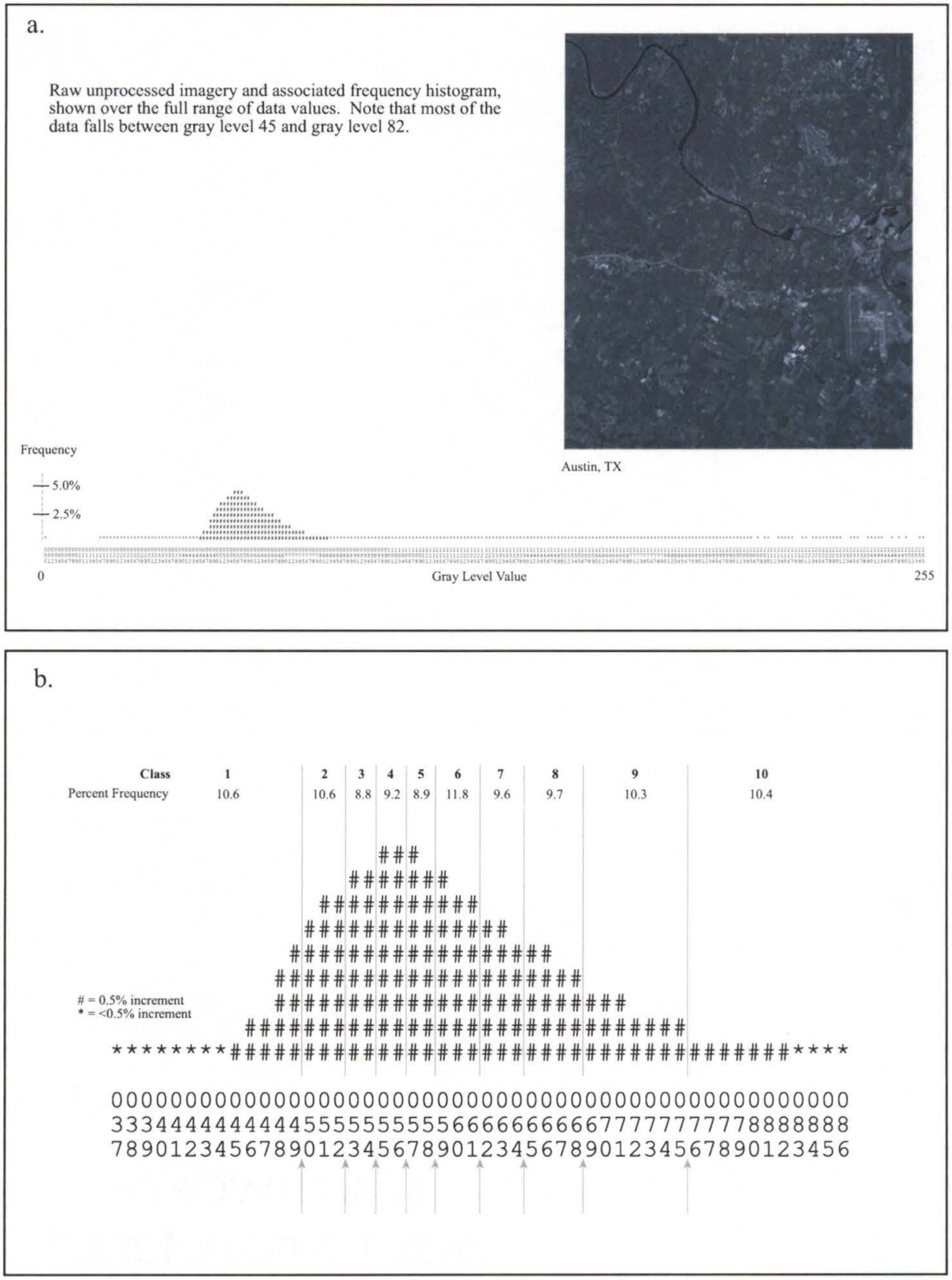

Figure 4. Raw image histogram (a) and sample one-dimensional classification scheme (b) for the Austin subset of the ETM+ panchromatic channel.

equal-interval classification would have been less effective because of the limited range of the majority of the data and the skewed nature of the data set as a whole. Further research could be done with regards to the use of other, more sophisticated means for choosing class limits. Note that due to the quantized, discontinuous nature of digital imagery, the data set cannot be divided exactly into equal-frequency classes. The discrete structure of the data dictates that some classes will have slightly more or less data than others. During the level slicing procedure illustrated in Figure 4, an attempt was made to minimize these differences by putting approximately 10 percent of the data in each of the ten classes. The actual frequencies of occurrence of each class for this example are listed in Figure 4b below the class numbers.

The radiometric resolution of the data in the panchromatic channel of this ETM+ scene was such that the maximum frequency of occurrence of pixels having any one particular gray level was approximately 5 percent (this number varies slightly from one subset to another). This means that the level slicing technique could divide the data into a maximum of 20 roughly equal frequency classes. In an attempt to generate as many classes as possible in the first-stage classification procedures, all 20 available equal frequency classes were used in generating the first-stage dasymetric image maps. The coarser system of 10 equal frequency classes, which is illustrated and discussed above, was found to be quite effective. However, the small amount of additional analysis required in generating a finer classification was judged to be well worth the incremental improvement in the precision of the level slicing procedure, and the corresponding improvement in the FBCC stage. This decision effectively doubles the data storage requirements for the frequency-based context matrices that are generated during FBCC (from 10 matrices to 20), which could present a potential problem depending on data storage space limitations.

Data Processing Procedures and Software

The construction of classified image maps from the satellite data was executed using primarily three software packages. ENVI®, developed by Research Systems, Inc., was used initially to perform image georeferencing and to interactively designate the dimensions of subsets of the ETM+ imagery. Terra Firma (Eyton 1999) was utilized in the actual subsetting of raw data and in performing all image classification procedures. The resultant classified image maps, output in raw form, were processed in Adobe Photoshop (developed by Adobe Systems, Inc.) for color indexing and conversion to TIFF files. ENVI® was then used again to georeference the TIFF files, allowing the final maps to be saved in a GEOTIFF format. This GEOTIFF format can easily be read into many common GIS software packages. For the purposes of this research, ENVI® was also used extensively in the interactive analysis of classification results. Finally, ENVI® was used to convert all maps and images to compressed GIF or JPEG files for incorporation into a graphics program and preparation for printing.

Table 3 lists the steps, including Terra Firma modules, which were employed in the processing of the FBCC panchromatic classification maps, from raw image data to GEOTIFF file preparation. Table 4 describes the various digital data files used or generated in the course of this procedure. The name 'subscene' is given to the sample image subset to denote a generalized example. This file structure was duplicated precisely for each classification that was undertaken. For the FBCC multispectral

Table 3. Steps for Generating an FBCC Panchromatic Classification Map

STEP	DESCRIPTION
1	Use the ENVI interface to determine the corner coordinates of the desired image subset in pixel lines and samples (rows and columns).
2	Create a subset in ENVI format, which generates a text header file containing the map coordination and projection information.
3	Use the SUBCON module of Terra Firma to perform subsetting of the raw data, using the pixel coordinates determined in step 1.
4	Run the COUNT module of Terra Firma on the subset to generate a histogram and frequency table.
5	Using the frequency table, determine the class limits necessary for an equal-frequency one-dimensional classification of the desired number of divisions. Create a text file of class limits, delineating these divisions.
6	Run the GRAY module of Terra Firma, using the class limits file, to level slice the data.
7	Import the raw image map into Photoshop for color table assignment and conversion to TIFF format.
8	Run the CONTXT2 module of Terra Firma on the raw image map generating frequency maps in band interleaved by line (BIL) format.
9	Run the TRAIN2 module of Terra Firma on the BIL frequency files to determine the optimal number of groups, select a training sample, and perform k-means cluster analysis.
10	Run the CLASS2 module of Terra Firma to complete the classification of the frequency-based contextual data by discriminant classification functions. Generate a classification statistics file.
11	Import the raw image map into Photoshop for color table assignment and conversion to TIFF format. Pad the TIFF file to make it the same raster size as the original subset.
12	Import the TIFF image maps into ENVI for georeferencing, using the text header created in step 2. The final products are GEOTIFF image maps of the first stage and the final stage of the classification procedure.

Table 4. Computer Files Utilized in the FBCC Processing of a Panchromatic Imagery Subset

FILE NAME	DESCRIPTION	FILE FORMAT
subscene.raw	Raw imagery (one byte per pixel)	binary raster
subscene.frq	Frequency table and histogram of raw data	ASCII text
subscene.img	ENVI image subset (contrast stretched)	ENVI standard
subscene.hdr	ENVI header file with map coordination and projection information	ASCII text
class1.cls	Raw data class assignment file	ASCII text
class1.raw	Classified image map (1 byte per pixel)	binary raster
class1.frq	Frequency table and histogram of class1.raw	ASCII text
class1.act	Indexed color table file	Adobe
class1.tif	RGB image map	TIFF
class1.hdr	ENVI header file with map coordination and projection information	ASCII text
context.grd	Class frequency maps (2 bytes per pixel), N grids for N classes, band interleaved by line (BIL)	binary raster
train2.rpt	Optimal groups statistics report	ASCII text
train2.dat	Training sample and cluster data	ASCII text
class2.raw	Contextually reclassified image map (1 byte per pixel)	binary raster
class2.frq	Frequency table and histogram of class2.raw	ASCII text
class2.rpt	Clustering and classification statistics report	ASCII text
class2.act	Indexed color table file	Adobe
class2.tif	RGB Image map	TIFF
class2.hdr	ENVI header file with map coordination and projection information	ASCII text

classification, Table 5 lists the processing steps employed and Table 6 describes the files that were used and created. As mentioned previously, the FBCC processing procedures for one-dimensional and multidimensional data are quite parallel. The primary difference between the two occurs in the first stage of classification, represented by steps 4 through 6 (Table 3) for the panchromatic classification and by steps 4 and 5 (Table 5) for the multispectral classification. Specifically for the multidimensional data processing (Table 5), note the similarity in procedure for the first stage classification, represented by steps 4 and 5, and for the second stage, represented by steps 8 and 9.

Map Legend Development

For each classified image map that was generated using the FBCC method, a map legend was developed by systematic interpretation of the thematic content of each class. This interpretive process was accomplished using two general steps. In the first step of legend development, the classes were examined in terms of the corresponding signatures present in the unprocessed or level sliced imagery. For the single-band classifications, an attempt was made in this first step to primarily judge the factors of pixel brightness and pixel heterogeneity within the assemblies of pixels making up the various classes. Color-mapped renditions of the level sliced data were useful in this segment of the analysis. For the multidimensional FBCC, an attempt was made in this step to assess the character of the various cover-types that were assembled into each class by examining the signatures found in a color infrared (CIR) composite (consisting of ETM+ bands 4,3, and 2 assigned to red, green, and blue respectively). The second step of legend development in both cases involved the interpretation of spatial variability and form, the integration of

Table 5. Steps for Generating an FBCC Multispectral Classification Map

STEP	DESCRIPTION
1	Use the ENVI interface to determine the corner coordinates of the desired image subset in pixel lines and samples (rows and columns).
2	Create a subset in ENVI format, which generates a text header file containing the map coordination and projection information.
3	Use the SUBCON module of Terra Firma to perform subsetting of the raw data, once for each of the six bands, using the pixel coordinates determined in step 1.
4	Run the TRAIN module of Terra Firma on the six bands of image data to determine the optimal number of groups, select a training sample, and perform k-means cluster analysis.
5	Run the CLASS module of Terra Firma to complete a per-pixel classification of the six-dimensional image data by discriminant classification functions. Generate a classification statistics file.
6	Import the raw image map into Photoshop for color table assignment and conversion to TIFF format.
7	Run the CONTXT2 module of Terra Firma on the raw image map, generating frequency maps in band interleaved by line (BIL) format.
8	Run the TRAIN2 module of Terra Firma on the BIL frequency files to determine the optimal numbers of groups, select a training sample, and perform k-means cluster analysis.
9	Run the CLASS2 module of Terra Firma to complete the classification of the frequency-based contextual data by discriminant classification functions. Generate a classification statistics file.
10	Import the raw image map into Photoshop for color table assignment and conversion to TIFF format. Pad the TIFF file to make it the same raster size as the original subset.
11	Import the TIFF image maps into ENVI for georeferencing, using the text header created in step 2. The final products are GEOTIFF image maps of the first stage and the final stage of the classification procedure.

Table 6. Computer Files Utilized in the FBCC Processing of a Six-Band Multispectral Imagery Subset (ETM+ XS bands 1-5 and 7)

FILE NAME	DESCRIPTION	FILE FORMAT
subscene.b1	Raw imagery (one byte per pixel), blue band	binary raster
subscene.b2	Raw imagery (one byte per pixel), green band	binary raster
subscene.b3	Raw imagery (one byte per pixel), red band	binary raster
subscene.b4	Raw imagery (one byte per pixel), near-IR band	binary raster
subscene.b5	Raw imagery (one byte per pixel), mid-IR band 1	binary raster
subscene.b7	Raw imagery (one byte per pixel), mid-IR band 2	binary raster
subscene.img	ENVI image subset containing all six bands (contrast stretched), band sequential (BSQ)	ENVI standard
subscene.hdr	ENVI header file with map coordination and projection information	ASCII text
train1.rpt	Optimal groups statistics report	ASCII text
train1.dat	Training sample and cluster data	ASCII text
class1.raw	Classified image map (1 byte per pixel)	binary raster
class1.frq	Frequency table and histogram of class1.raw	ASCII text
class1.act	Indexed color table file	Adobe
class1.tif	RGB image map	TIFF
class1.hdr	ENVI header file with map coordination and projection information	ASCII text
context.grd	Class frequency maps (2 bytes per pixel), N grids for N classes, band interleaved by line (BIL)	binary raster
train2.rpt	Optimal groups statistics report	ASCII text
train2.dat	Training sample and cluster data	ASCII text
class2.raw	Contextually reclassified image map (1 byte per pixel)	binary raster
class2.frq	Frequency table and histogram of class2.raw	ASCII text
class2.rpt	Clustering and classification statistics report	ASCII text
class2.act	Indexed color table file	Adobe
class2.tif	RGB Image map	TIFF
class2.hdr	ENVI header file with map coordination and projection information	ASCII text

reference information (field survey for ground truth, DOQQ imagery, other existing maps) and, most importantly, the consideration of the geographic context of the classes. The goal of the legend development process was to obtain a description of each of the contextually reclassified map units in terms of physical and/or human geography. As an intermediate step in the process, it was useful to look at various georegistered "paint chips" taken directly from the digital imagery, showing the relationship of the unprocessed imagery with the results of the first, per-pixel step of image classification and the results of the second, frequency-based contextual step of image classification.

The use of the ENVI® GIS/Remote Sensing software was instrumental in developing a geographic information system to display and analyze the imagery and classified image maps. In order to assimilate the information gained during field survey, the position coordinates of ground locations were located and used as a basis for examination of the imagery, allowing a vertical view and a ground view at the same time. This analysis proved highly effective in facilitating visualization of the information in the satellite imagery. The knowledge gained by the interpreter during the analysis of an automated classification can lead to a much more sophisticated interpretation than simpler, photo-interpretation methods of classification. ENVI® permits the user to view the imagery and an associated classified image map simultaneously, with a spatial link established between the two. This instant georegistration of imagery to image map was crucial in the legend development phase of the classification procedure.

Classification Comparative Analysis and Post-Processing

A qualitative assessment of the experimental panchromatic FBCC classification technique was made through a direct comparison with the results of the more established multispectral FBCC classification system. The results of the panchromatic image classification for the Austin subset were evaluated in terms of the similarities and differences to the patterns that were derived using a multispectral FBCC classification. This comparison was useful in making an overall assessment of the strengths and weaknesses of the untried technique.

As a final processing step, a class merging procedure was performed on one of the panchromatic FBCC maps as a simple demonstration of the technique. The goal of class merging in general was to achieve a classification system that maximized utility for land use/land cover mapping, while minimizing the kernel-related boundary effect that is known to occur with frequency-based contextual classification (Eyton 1993). Class merging was based in part on the spatial properties of the various classes, i.e., by looking for classes that were obvious "boundary" classes. This common procedure was accomplished by using Photoshop to assign the same index color values to the classes for which merging was desired, and generating a new TIFF file to reflect the changes.

Field Survey

Ground truthing was performed at several locations throughout the study area to assist in the process of creating a legend for the classified image maps, and to qualitatively assess the viability of the experimental panchromatic classification system. The ground checking was accomplished by conducting a simple field survey, the goal of which was to gather a base of useful reference data on the character of the ground cover in various parts of the study area. The information gained in ground survey was then used in validation of the classes found in the automated pattern recognition. The point of this survey was not to systematically obtain field checks of every part of the scene, but rather to obtain a set of high-quality, high confidence information that could be of use in evaluating the strengths and weaknesses of the experimental data processing procedure. Since the survey was conducted mainly in the spring of 2000, five months after satellite image acquisition, it did not have the capability of validating phenomena that were time-critical.

A handheld GPS unit and magnetic compass were used to collect the data, in conjunction with a digital camera (in some cases, a film camera was used to make negatives which were then scanned using a Polaroid SprintScan 35 Plus film scanner). Locations were chosen with the intention of obtaining photos of a variety of ground cover types, although this was problematic due to the inaccessibility of many areas and due to limitations in time and resources. Several pictures were collected at each location, along with general notes about the ground features located at the site and a GPS position reading. The GPS data collected, although not differentially corrected, did allow for rapid map coordination of field survey locations (FSLs) using the GIS system described above. Each picture that was taken was accompanied by an azimuth reading from the compass, to allow a reconstruction of the line of sight of the photo when looking at the satellite imagery.

CHAPTER V

RESULTS AND DISCUSSION

FBCC Kernel Size Experiment

Before the final FBCC image maps were produced, preliminary experimentation was done to determine the appropriate kernel size to be used in the extraction of context information. Figure 5 illustrates the results of this experiment. A single portion of the panchromatic imagery (Austin subset) was classified using kernel sizes of 7x7 pixels (Figure 5a), 15x15 pixels (Figure 5b), and 31x31 pixels (Figure 5c). The results of this experiment can be compared in terms of the evidence of the boundary effect, the level of generalization of the map, and the overall appropriateness of the various kernel sizes for the intended purpose of mapping land use and land cover with imagery of this resolution in an urban and suburban setting. Each of these sample classifications was performed using the previously outlined technique for finding the optimum number of natural groups, which generated different groupings for each example. Thus the three examples were not directly comparable in terms of the number or content of classes.

The classified regions in Figure 5b, derived using a 15x15-pixel kernel size, had a much more generalized appearance than those in 5a which were derived using a 7x7 kernel. The boundary effect was also more evident in 5b, but this was probably related to the fact that the number of natural groups used in the classification (based upon the a.

b.

c.

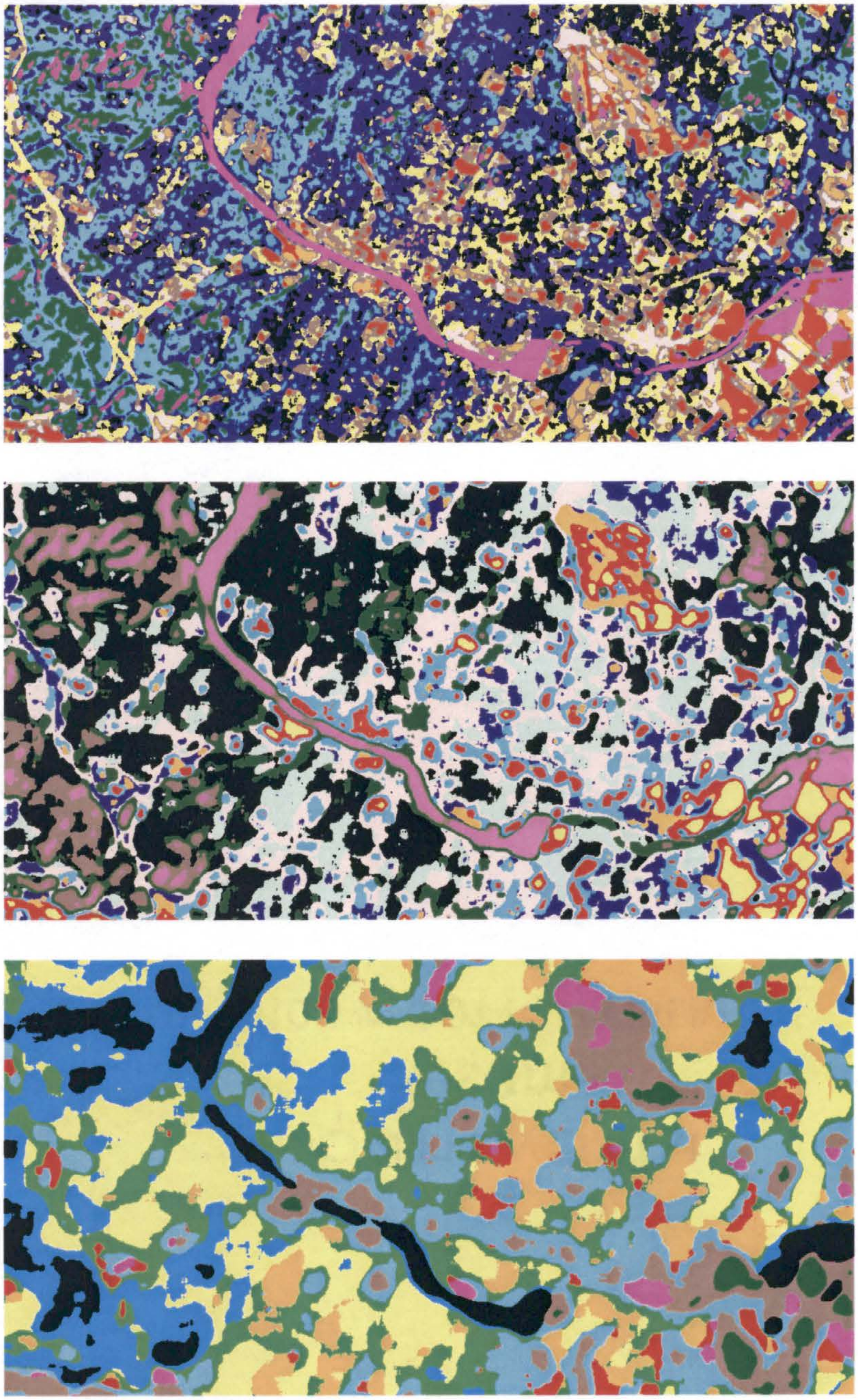

Figure 5. Comparison of kernel sizes for classification of panchromatic data. 7x7 kernel (a), 15x15 kernel (b), 31x31 kernel (c). Austin's Town Lake is the large linear feature in the center of each scene.

results of the F-ratio test) was higher. The increase in boundary effect was not necessarily considered to be problematic in a classification, as the application of class merging should provide a relatively easy way of dealing with the boundary problem, should it arise. Overall, the patterns that were recognized using the 15x15 kernel size (Figure 5b) were quite similar to those found using the 7x7 (Figure 5a), but the classification in 5b had more of an amorphous, "blob-like" appearance, rendering the spatial structure of the urban scene more difficult to recognize and interpret. This problem was even more dramatic with the use of a 31x31-pixel kernel, illustrated in Figure 5c, in which the shapes of the classes have been generalized almost to abstraction.

Based upon the results of the experiment, a kernel size of 7x7 pixels was selected for the FBCC processing of the panchromatic data set. This assessment was based in part on a study done by Eyton (1993), with data of 7.5 meters resolution. In that case, a kernel size of 15x15 pixels was established as the minimum at which the information that was extracted could be expected to differ appreciably with a decrease in the size of the kernel. Another factor to consider is that the dimensions of a city block form a logical minimum spatial unit for classification of an urban scene. With the ETM+ panchromatic imagery, a kernel size of 7x7 pixels corresponds to a ground area of 105 meters square as the unit of analysis for the extraction of context information (an acceptable approximation of the dimensions of a typical city block). The classification that was processed with a 7x7 kernel size, compared to the other two more generalized examples (Figure 5), more effectively preserved linear features such as streets and roads and seemed to give a better sense of the structure of regular spatial patterns in the scene.

The 7x7 kernel size was again utilized in the FBCC processing of the multispectral scene. The multispectral data were of 30 meters resolution, effectively doubling the square dimensions of the unit of context analysis for the multispectral classification compared to the panchromatic. Although this was problematic in terms of making a direct comparison between the two, this decision was viewed as a necessary compromise. At kernel sizes of less than 7x7 pixels, the number of pixels in the context measure becomes exceedingly small and it could become difficult to differentiate meaningful clusters from the context data, especially given the aspatial, frequency-based method of extracting the context matrices. In the final analysis, the decision of what kernel size to use in FBCC classification is dependent primarily on the type of land cover and land use which is to be classified and on the desired scale of analysis. Obviously this consideration would be different for classification of an urban scene than for classification of other geographic areas such as natural vegetation cover or land use units associated with large-scale forestry.

FBCC Image Maps from Panchromatic Imagery

The image maps shown in Figure 6 (Austin) and Figure 7 (San Marcos) show the results of the application of the FBCC classification procedures to the panchromatic band of ETM+ data. The detailed results of the unsupervised legend development for Figures 6 and 7 are presented in Table 7 using the two-stage format that is outlined above. The relative frequencies of class occurrence for the two maps are given in Table 8 (Austin) and 9 (San Marcos). As mentioned previously, the first-stage, level slicing step for both classifications was accomplished by dividing the data into 20 equal-frequency divisions.

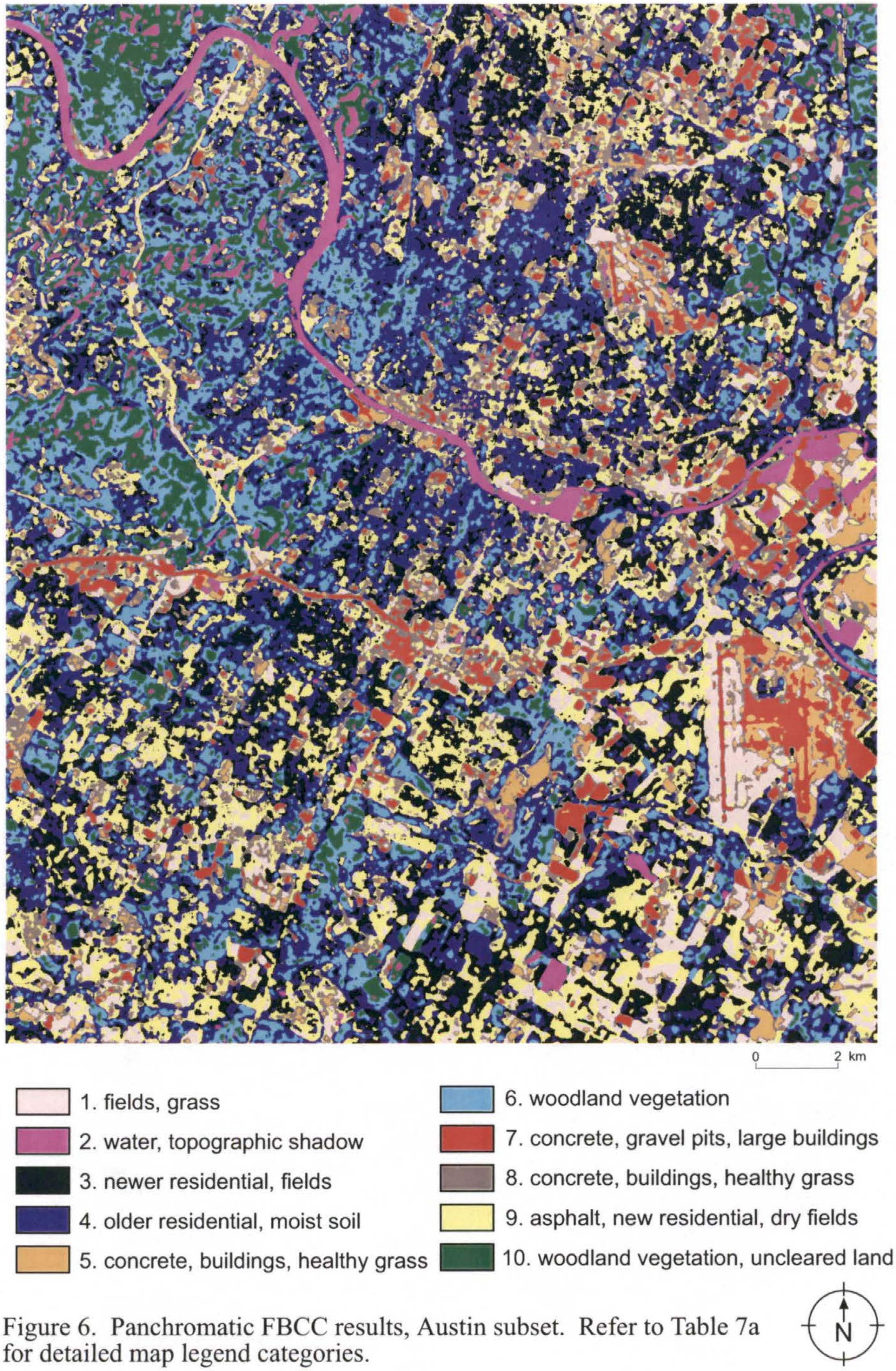

Figure 6. Panchromatic FBCC results, Austin subset. Refer to Table 7a for detailed map legend categories.

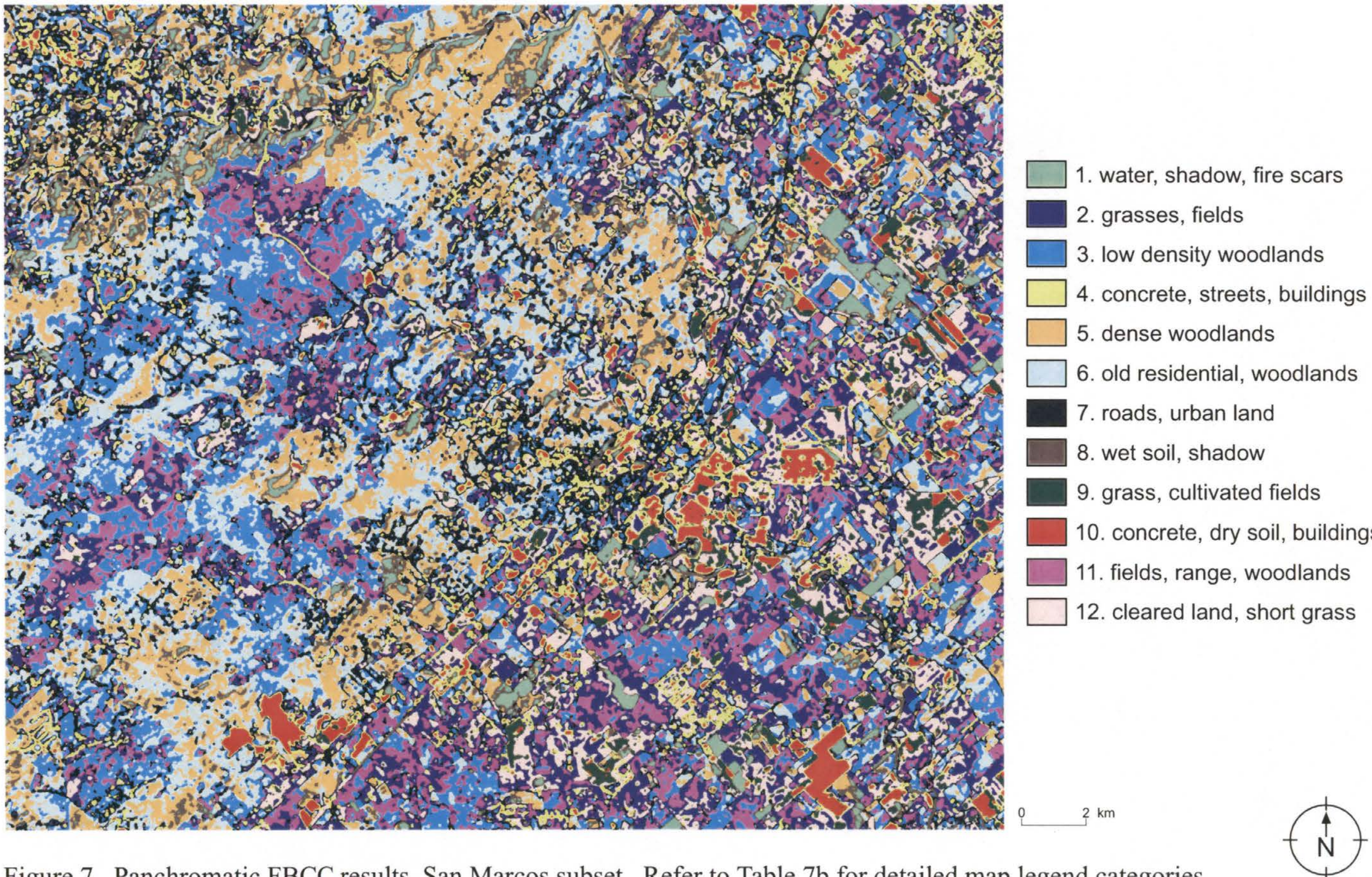

Figure 7. Panchromatic FBCC results, San Marcos subset. Refer to Table 7b for detailed map legend categories.

Table 7. Panchromatic FBCC Legend Development, Austin and San Marcos Subsets

7a. AUSTIN SUBSET		
CLASS #	STEP 1: SIGNATURE	STEP 2: LAND USE/LAND COVER
1	medium-bright, heterogeneous	lawns, fields, large areas of grass
2	very dark, homogeneous	water, topographic shadow, wet soil
3	medium, heterogeneous	residential with sparse trees, fields (a mixed class)
4	medium-dark, heterogeneous (similar to 3)	older residential with trees, range that has been cleared, somewhat moist soil
5	medium-bright, homogeneous	concrete, gravel pits, large buildings, very dry soil, healthy grass (golf courses)
6	dark, heterogeneous (edge of 10)	natural woodland vegetation
7	brightest, homogeneous	clean, dry concrete, large extractive processes, large buildings
8	medium-bright, heterogeneous (edge of 5)	concrete, large buildings
9	medium, heterogeneous (similar to 3)	asphalt, residential with sparse trees, dry fields
10	dark, heterogeneous	natural woodland vegetation, uncleared land
7b. SAN MARCOS SUBSET		
CLASS #	STEP 1: SIGNATURE	STEP 2: LAND USE/LAND COVER
1	darkest, homogeneous	water, topographic shadow, plowed fields, fire scars
2	medium, heterogeneous	grasses, cleared range, agricultural fields (similar to 11)
3	medium-dark, heterogeneous	low density woodland vegetation, older residential with trees, partially cleared range, fields (a mixed class)
4	bright, homogeneous	concrete, roofs, buildings, streets (edge of 10)
5	dark, heterogeneous	dense woodland vegetation
6	medium-dark, heterogeneous	woodland vegetation, older residential with trees (edge of 5)
7	medium-bright, heterogeneous	highways, roads, urban and built up land
8	dark, homogeneous	topographic shadow, wet soil, fire scars (edge of 1)
9	bright, heterogeneous	cultivated fields, bare soil, grass (similar to 12)
10	brightest, homogeneous	gravel pits, extremely dry soil and clean concrete
11	medium-dark, heterogeneous	mixed range and woodlands, soil, agricultural fields (similar to 2)
12	medium-bright, heterogeneous	cleared rangeland, dry fields and soil, short dry grasses (similar to 9)

Table 8. One-Dimensional FBCC Class Frequencies and GLV Boundaries, Austin Subset

STAGE 1: LEVEL SLICING			
CLASS #	CLASS %	ACCUMULATED %	GLV RANGE
1	4.580	4.580	0 - 46
2	6.033	10.613	47 - 49
3	6.643	17.256	50 - 51
4	3.993	21.249	52
5	4.267	25.516	53
6	4.490	30.005	54
7	4.592	34.597	55
8	4.589	39.187	56
9	4.533	43.040	57
10	4.371	48.090	58
11	4.187	52.277	59
12	7.649	59.926	60 - 61
13	3.436	63.362	62
14	6.152	69.514	63 - 64
15	5.264	74.778	65 - 66
16	4.476	79.254	67 - 68
17	5.371	84.625	69 - 71
18	4.932	89.556	72 - 75
19	5.451	95.007	76 - 83
20	4.993	100.000	84 - 256
STAGE 2: FBCC			
CLASS #	CLASS %	----------------------	----------------------
1	4.584	----------------------	----------------------
2	3.027	----------------------	----------------------
3	15.183	----------------------	----------------------
4	24.819	----------------------	----------------------
5	2.687	----------------------	----------------------
6	11.743	----------------------	----------------------
7	4.314	----------------------	----------------------
8	11.204	----------------------	----------------------
9	16.533	----------------------	----------------------
10	5.906	----------------------	----------------------

Table 9. One-Dimensional FBCC Class Frequencies and GLV Boundaries, San Marcos Subset

STAGE 1: LEVEL SLICING			
CLASS #	CLASS %	ACCUMULATED %	GLV RANGE
1	4.661	4.661	0 - 48
2	4.479	9.140	49 - 50
3	6.817	15.957	51 - 52
4	4.085	20.042	53
5	4.422	24.463	54
6	4.659	29.122	55
7	4.795	33.917	56
8	4.843	38.760	57
9	4.879	43.640	58
10	4.840	48.480	59
11	4.763	53.243	60
12	4.657	57.900	61
13	4.535	62.435	62
14	8.360	70.795	63 - 64
15	3.697	74.492	65
16	6.260	80.752	66 - 67
17	4.780	85.532	68 - 69
18	5.106	90.639	70 - 72
19	4.793	95.432	73 - 78
20	4.568	100.000	79 - 255
STAGE 2: FBCC			
CLASS #	CLASS %	---------------------	---------------------
1	1.943	---------------------	---------------------
2	9.721	---------------------	---------------------
3	15.334	---------------------	---------------------
4	5.921	---------------------	---------------------
5	10.820	---------------------	---------------------
6	16.011	---------------------	---------------------
7	15.214	---------------------	---------------------
8	4.890	---------------------	---------------------
9	2.340	---------------------	---------------------
10	2.364	---------------------	---------------------
11	8.932	---------------------	---------------------
12	6.511	---------------------	---------------------

In the Austin map (Figure 6) the second-stage, FBCC procedure produced 10 classes. The FBCC produced 12 classes in the San Marcos map (Figure 7). The overall correct classification of the training data during FBCC was 95.80% for the Austin map and 96.15% for the San Marcos map. Training sample sizes were 1763 and 1558 pixels, respectively.

Representative sub-areas of each of the two data subsets have been isolated, magnified, and displayed using a series of georegistered images in order to further illustrate the process of assigning a legend to the image maps. These series (Figure 8 for Austin and Figure 9 for San Marcos) also serve to demonstrate the processing stages of the single-band classification. The image in Figure 8a is a contrast stretched rendition of a part of the raw panchromatic imagery used in the classification of the Austin subset. The image in Figure 8c is a spectral-sequence rendition of the 20 level slices making up the first stage of the classification process. The darkest slice was assigned to blue, and the brightest slice was assigned to red. The use of this spectral sequence allowed an effective visualization of the overall relative brightness or darkness of the assemblies of pixels in various portions of the subset area. The image in Figure 8b is similar to Figure 8c, except that the level slices were assigned to random colors (and only 10 equal-frequency level slices were used for this rendition). This color scheme allowed an effective visualization of the homogeneity or heterogeneity of the various assemblies of pixels in the subset. Figure 8d is taken from the fully processed classification image map (corresponding to Figure 6 and Table 7a), and is included for reference to the spatial arrangement and areal extent of each of the classes. This same illustrative series is

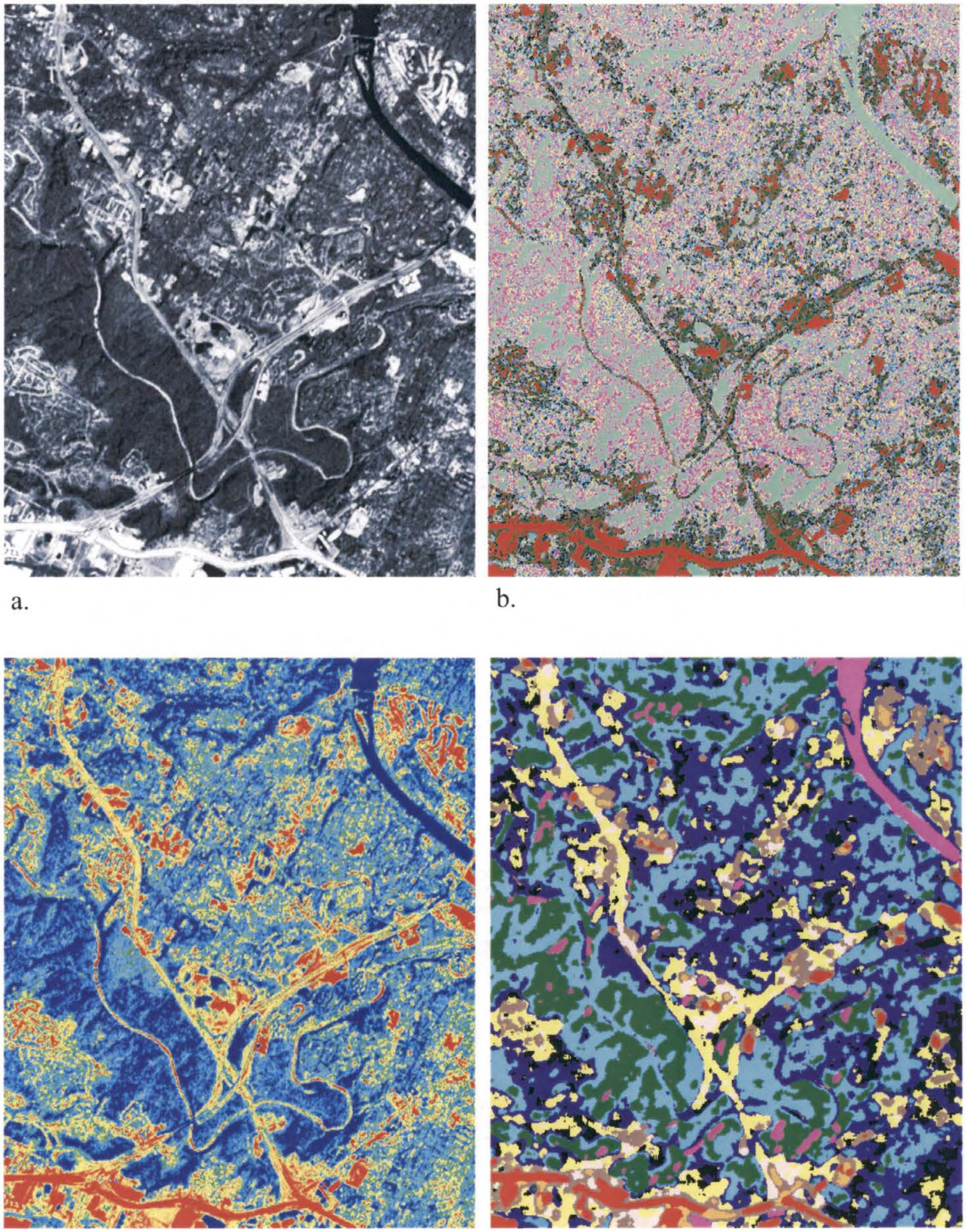

a. b.

c. d.

Figure 8. Detail of panchromatic FBCC, Austin subset. Contrast stretched image (a), level sliced image, random colors (b), level sliced image, spectral colors (c), and FBCC image map (d). This figure depicts a subset of Figure 6.

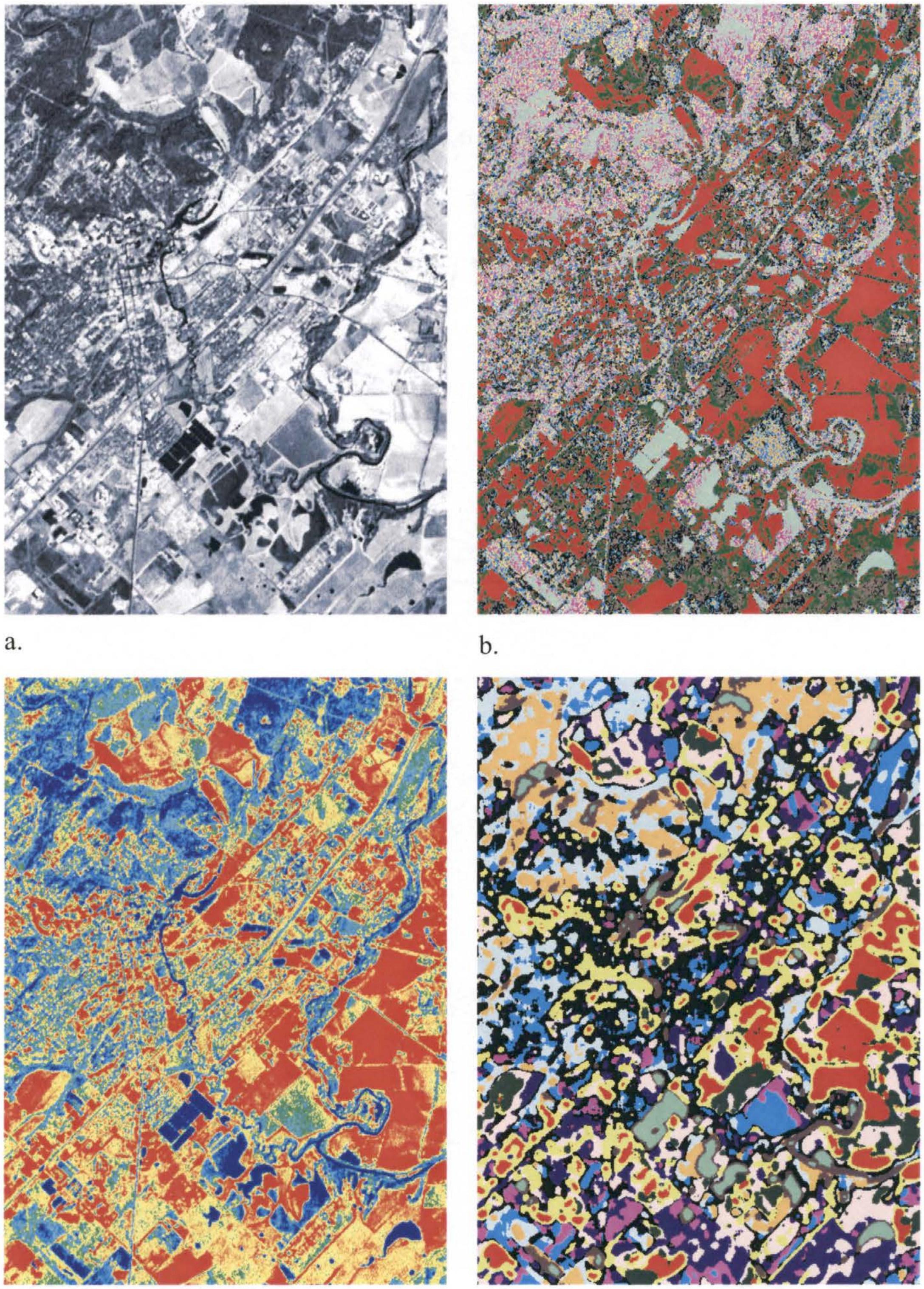

Figure 9. Detail of panchromatic FBCC, San Marcos subset. Contrast stretched image (a), level sliced image, random colors (b), level sliced image, spectral colors (c), and FBCC image map (d). This figure depicts a subset of Figure 7.

repeated for the San Marcos study area in Figure 9 (corresponding to the map given in Figure 7 and the legend given in Table 7b).

Examination of this set of images for the panchromatic FBCC classifications was the primary tool for analysis in the first stage of legend development. As discussed previously, the interactive linked display capabilities of the ENVI® software allowed this detailed analysis to take place over the entire extent of the two study areas, preempting the need to subset the data as has been done for illustration here. By isolating the spatial and spectral "signature" characteristics of each class in the FBCC image map, the analyst is able to attempt a systematic determination of thematic content.

The challenge to the analyst is that these signatures alone do not always fully segregate themselves into meaningful land cover or land use types that apply universally to the entire scene being classified. In most cases, a particular class can represent different things on the ground depending on its geographic context and occasionally depending on time-critical factors unique to the image being analyzed. This general weakness of automated image classification can be particularly problematic for the single-band technique that is explored in this paper.

In the single band of the ETM+ panchromatic channel, the radiation that is recorded extends into the near-IR wavelengths. Therefore vegetation type, vegetation vigor, and dryness or moistness of the soil or other ground surfaces will have a significant impact on pixel response and thus on the outcome of the single-band classification, due to the sensitivity of the IR reflectance to each of these factors. These factors had to be adequately considered during the process of developing a map legend for the FBCC, along with other important factors such as the presence or absence of highly reflective impermeable ground cover (concrete, roofs of large buildings), of medium reflectance impermeable surfaces such as asphalt and shingled roofs, and of other ground cover types. The amount and type of vegetation present in an urbanized area will greatly affect its class assignment, allowing a degree of differentiation between older, more established residential neighborhoods, newer neighborhoods with less abundant or less mature trees, and commercial or industrial areas that are typically composed mainly of impermeable ground cover. This differentiation was certainly present in the results of the classifications discussed here.

Comparison of Multiband and Single-Band FBCC Image Maps

The classified image map in Figure 10 shows the results of the application of the FBCC technique to the six multispectral bands of the ETM+ data for the Austin subset. The detailed results of the two-stage legend development are given in Table 10, and the class frequencies are given in Table 11. The per-pixel classification produced an overall correct classification for the training field data of 93.68%, with a sample size of 2736 pixels. In the FBCC stage, the overall correct classification was 97.00%, again with a sample size of 2736 pixels. As explained previously, the first stage of legend development for the multispectral classification was accomplished by examining a color infrared composite of the unprocessed imagery, and a kernel size of 7x7 pixels was used to extract the frequency-based context matrices. In this case, only 10 matrices were extracted, corresponding with the 10 natural groups that were found in the first-stage, per-pixel classification procedure. In the 10-group classification used as a basis for extraction of context information from the multispectral data, the grouping did not

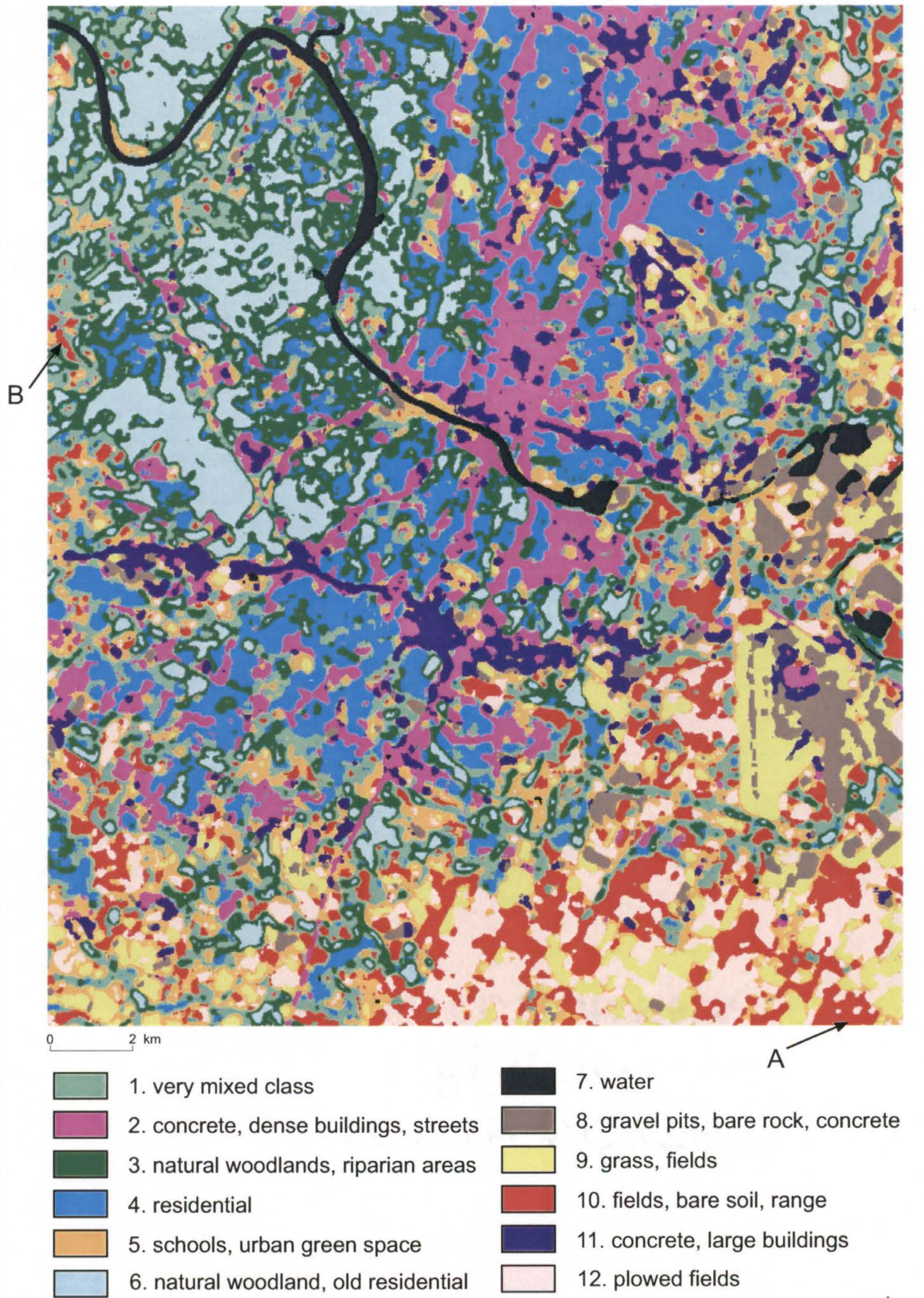

Figure 10. Multispectral FBCC results, Austin subset. Refer to Table 10 for detailed map legend categories.

Table 10. Multispectral FBCC Legend Development, Austin Subset

CLASS #	STEP 1: CIR SIGNATURE	STEP 2: LAND USE/LAND COVER
1	red, bright red	natural vegetation (a very mixed class)
2	cyan	concrete, buildings, streets, central business district, new residential (few trees)
3	dark red	natural woodland vegetation, riparian systems
4	dark red with cyan lines	residential with trees (older residential than class 2)
5	bright red, white, greenish brown	schools, golf courses, urban green space (a mixed class)
6	dark red	natural woodland, old residential (dense trees)
7	black, dark blue	water
8	white, light brown	gravel pits, large areas of dry bare concrete or rock
9	light brown, light red, pink	grass, fields
10	dark brown, dark cyan, dark red	bare soil, range, fields
11	white, cyan	large buildings, concrete, extensively developed land
12	dark cyan, brown, greenish brown	plowed fields

Table 11. Multispectral FBCC Classification Results: Class Frequencies, Austin Subset

STAGE 1: PER-PIXEL CLASSIFICATION		STAGE 2: FBCC	
CLASS #	CLASS %	CLASS#	CLASS %
1	3.286	1	13.300
2	14.690	2	10.959
3	7.968	3	14.929
4	1.551	4	12.897
5	1.595	5	10.307
6	13.371	6	8.442
7	10.520	7	1.915
8	19.799	8	3.694
9	4.957	9	5.032
10	22.263	10	7.399
		11	5.695
		12	5.430

involve equal-frequency classes as in the single-band examples (nor was this expected). The multispectral FBCC map in Figure 10 can be compared to Figure 6, the panchromatic FBCC covering the same geographic area.

These two classification maps are shown together in Figure 11 for comparative purposes along with the unprocessed pan imagery and the color infrared composite of the multiband imagery. Examination of the Austin multispectral image composite and corresponding FBCC image map indicated that this conventional, multiband application of the technique had some notable differences from the experimental panchromatic classification system. As was expected, the multispectral classification was able to more readily distinguish between natural vegetation and agriculture, as well as between agriculture and bare soil, compared to the panchromatic. This is demonstrated by the existence of separate vegetation classes in the agricultural areas (the south and southeast portions of the Austin scene) from those classes delineating areas of natural woodland vegetation. In the panchromatic classification, there was a greater amount of classification overlap between agricultural areas and natural woodland areas, as these two land cover types more frequently fell into the same class. However, the multispectral FBCC was not immune to this problem, and a certain amount of ambiguity still existed as to the meaning of the various classes. The results from the multiband FBCC demonstrated again that classes could be expected to be associated with different land uses, dependent upon the geographic context.

Classes 1, 5 and 10 in the multiband FBCC were particularly difficult to interpret. Class 10, as an example, represents areas of plowed fields in one part of the scene (Figure 10, location A) and the patches of rough in a golf course in another part (Figure 10,

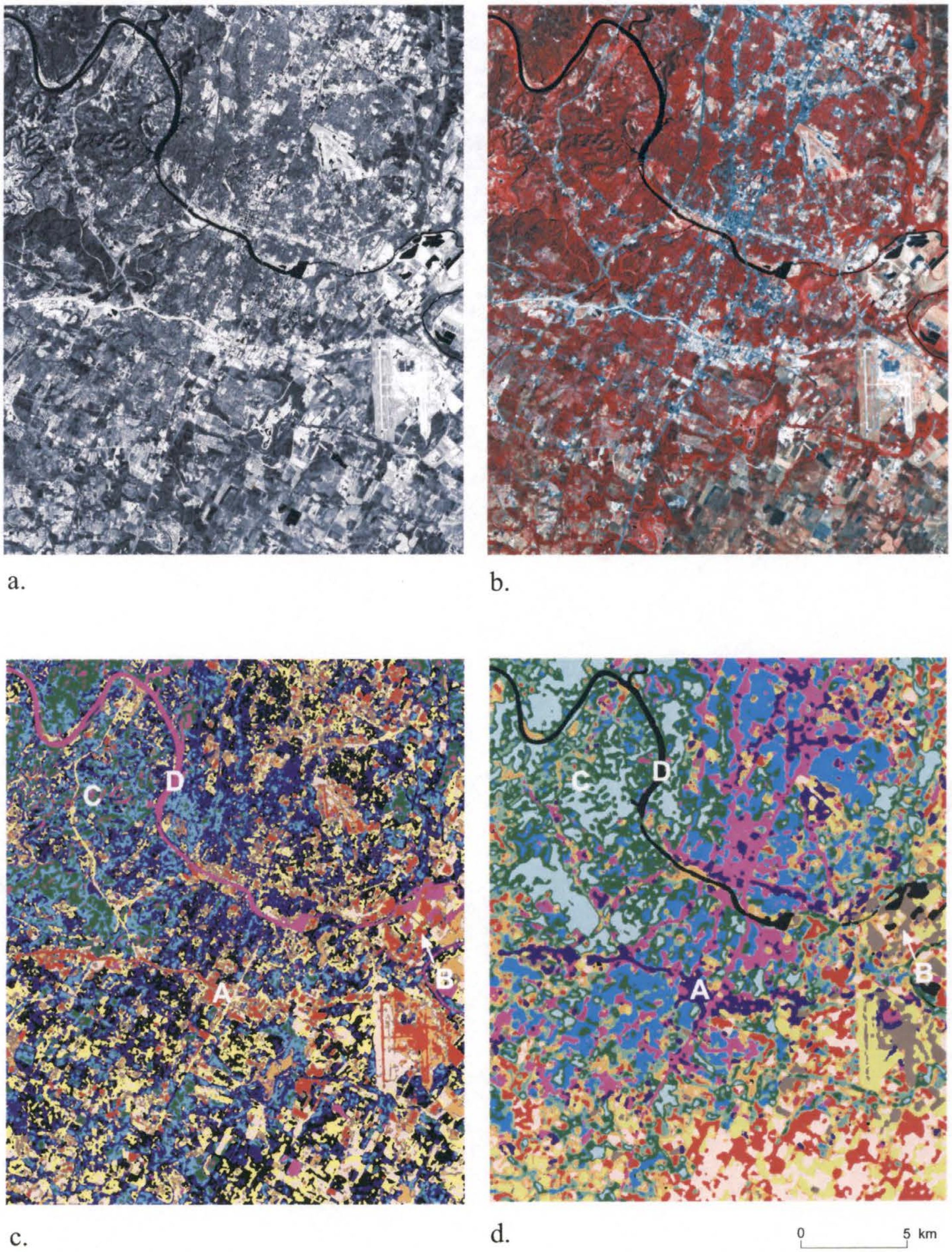

Figure 11. Comparison of panchromatic and multispectral FBCC Results, Austin subset. Pan imagery (a), CIR (4-3-2) composite (b), pan FBCC map (c), multispectral FBCC map (d). For map legends of (c) and (d), see Figures 6 and 10.

location B). With 6 bands of multispectral data, the interpretation of the FBCC became quite complex. Since the analyst could only consider three bands of data at a time in the form of an image composite, difficulties often arose with interpretation of the classification in terms of CIR signatures: two areas falling in the same class might present completely different signatures in terms of what can be seen in a CIR composite, but presumably were similar enough in the other bands to be grouped together by the classifier. An examination of several different composites and/or of the results of the per-pixel classification step may be helpful in future analyses. The primary strength of a multispectral FBCC compared to a panchromatic one was that the multispectral procedure increased the separability of areas that might have been grouped together in the panchromatic classification due to their similarity of spectral response in the single-channel image. Prominent examples of this are high-density urban concrete structures and buildings (Figure 11, location A) vs. dry bare soil (Figure 11, location B) and topographic shadow (Figure 11, location C) vs. deep water (Figure 11, location D).

Upon detailed examination, the patterns seen in the panchromatic and multispectral FBCC image maps were found to be remarkably similar overall in terms of the information that they can provide to the interpreter. Also evident with detailed study of these classification systems is the fact that automated classification, whether involving single-band or multiband imagery, is certainly not a simple input/output process. The true value of the FBCC classification technique is in its capacity to highlight the areas of similar spectral and contextual characteristics in the image. It is very much up to the interpreter to decide whether this constitutes grounds for placing various areas in the same land cover or land use class.

Analysis of Field Survey Results

Ground-based photography was used as an adjunct to and a validation of the systematic approaches described above for the interpretation of the thematic content of the FBCC maps. In total, over 140 photos were obtained at 55 sites, with 24 sites in the Austin study area and 31 sites in the San Marcos study area. Acquisition dates ranged from mid February to mid March of 2000. The distribution of the entire set of field survey locations (FSLs) has been plotted over the contrast stretched panchromatic imagery in Figures 12 (Austin) and 13 (San Marcos). The selection of photos that is described in detail here is included as a representative sample of the way in which this type of ground truth information can be indispensable in facilitating the interpretation of classification results. Each photo was accompanied by an azimuth reading, recorded at the time the photo was taken, to aid in relation of the visual information present in the photo with the vertical view afforded by the satellite image and classification map.

Figures 14, 15, and 16, which are discussed in detail below, each contain four ground photos (c through f) along with a small piece of the satellite imagery (a) and the classification map (b). North (azimuth 000) is to the top of the page for the satellite imagery and image maps in each of these three figures. A compass rose is included in each figure for easy reference when using the azimuth information. The FSLs were located on the ETM+ imagery primarily by the use of readings from a handheld GPS receiver. Since the readings were not differentially corrected, precluding precise automatic position location of the FSLs in the ETM+ imagery, DOQQ imagery of 2.5 meters resolution was used as a guide for position location when necessary.

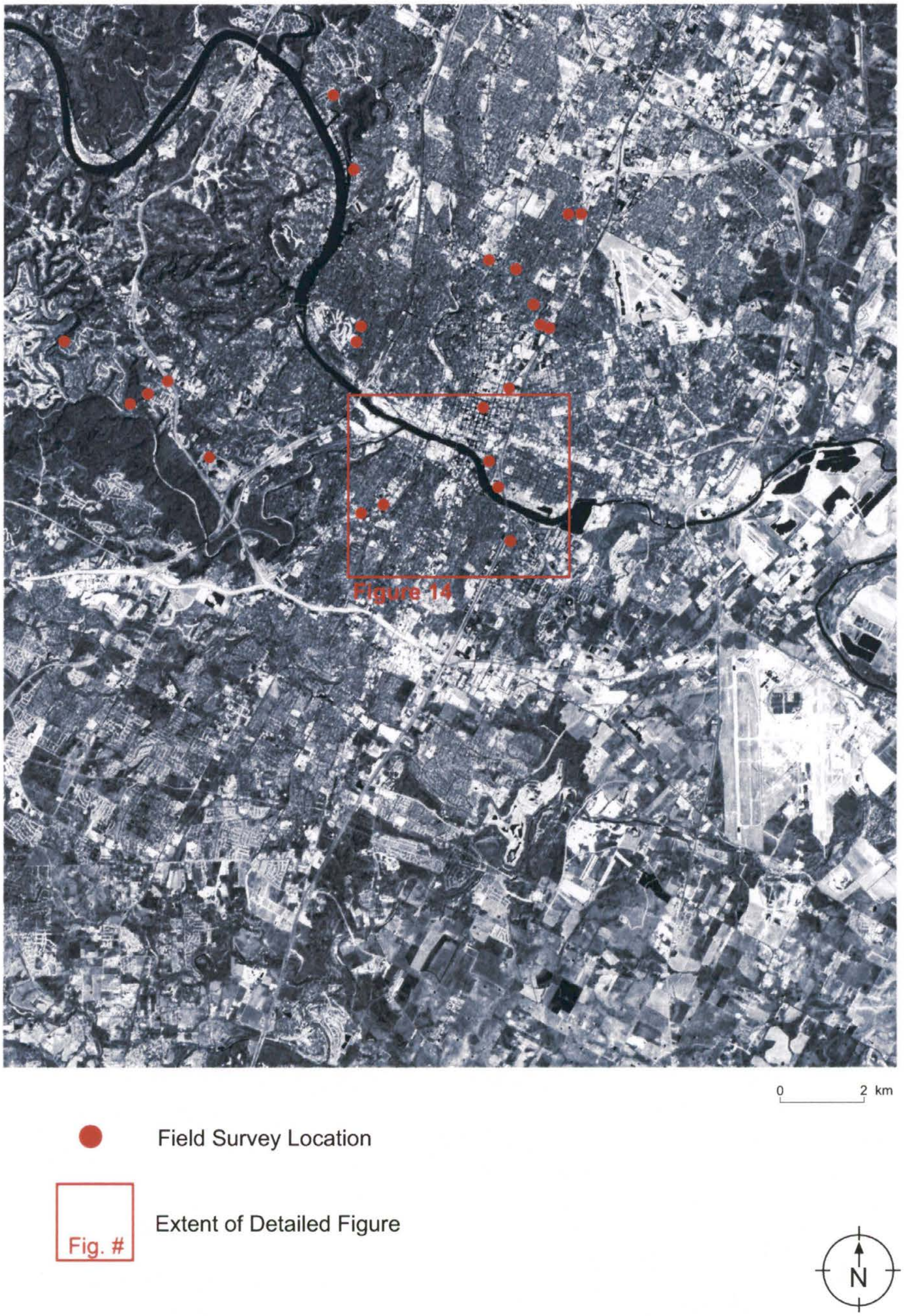

Figure 12. Field survey locations plotted on contrast stretched panchromatic imagery, Austin subset.

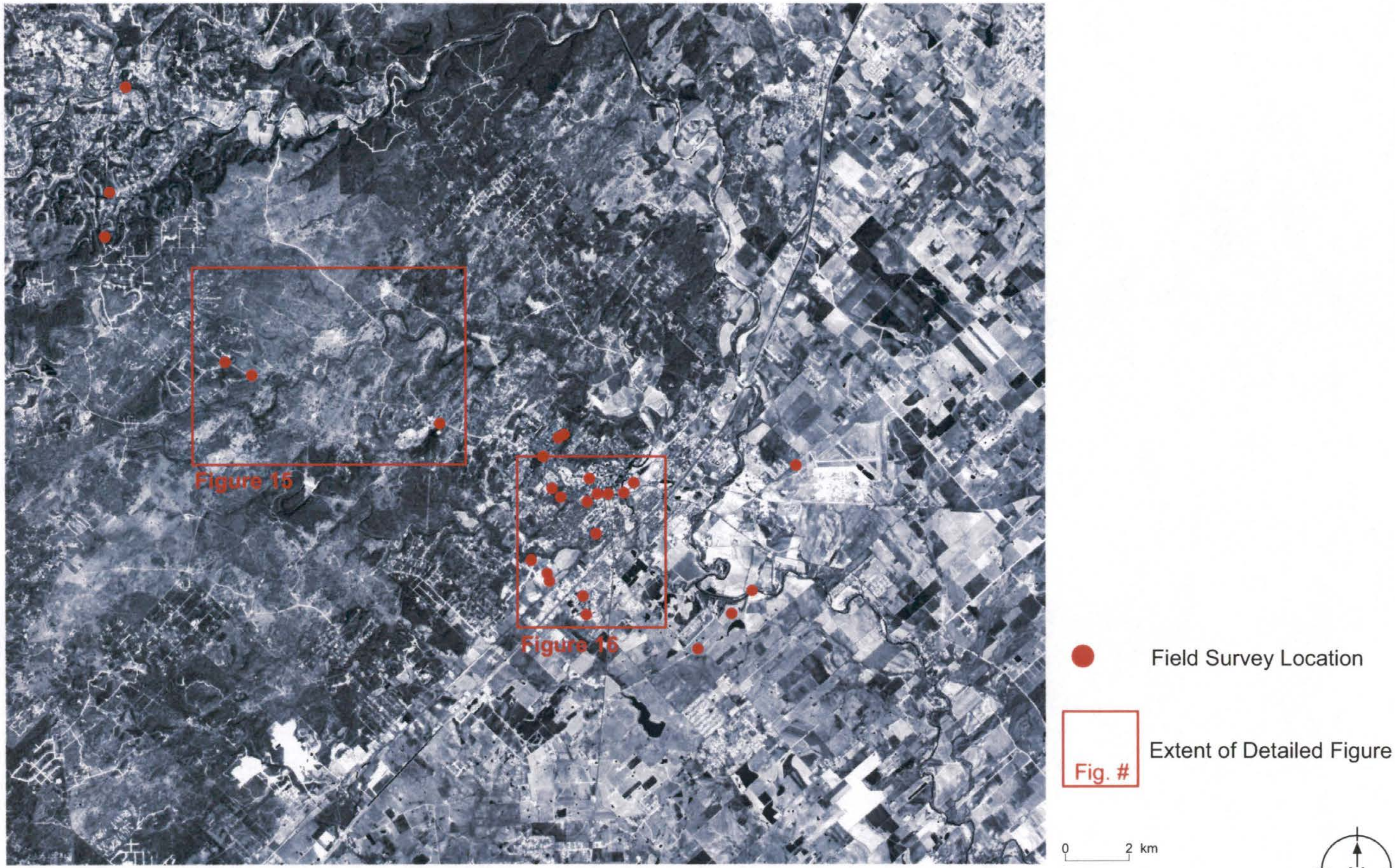

Figure 13. Field survey locations plotted on contrast stretched panchromatic imagery, San Marcos subset.

a.

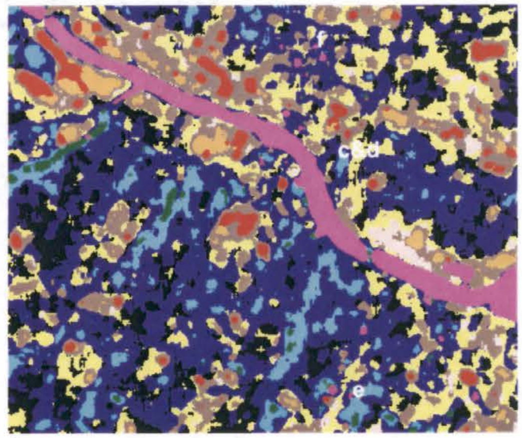

b.

c. Azimuth = 282 degrees

d. Azimuth = 316 degrees

e. Azimuth = 352 degrees

f. Azimuth = 026 degrees

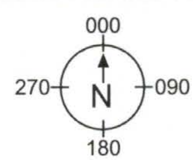

Figure 14. Ground truth examples in the vicinity of downtown Austin. See text for descriptions. Compass rose is for use with (a) and (b).

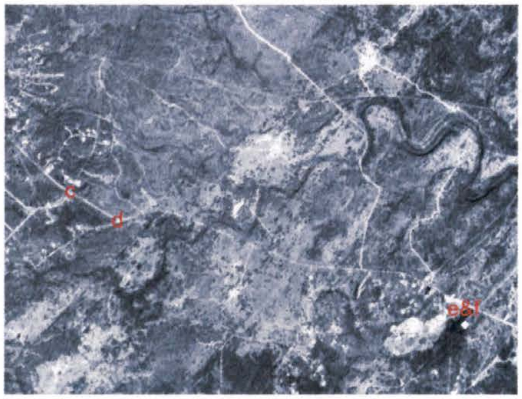

a.

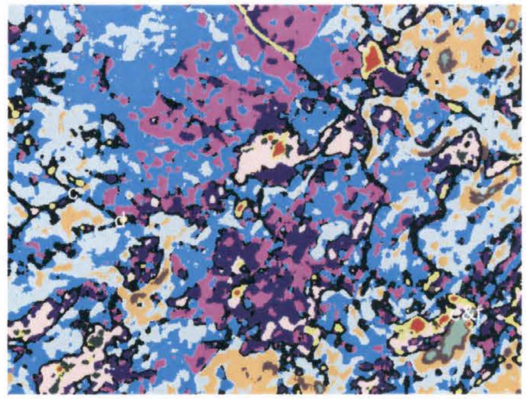

b.

c. Azimuth = 230 degrees

d. Azimuth = 310 degrees

e. Azimuth = 315 degrees

f. Azimuth = 180 degrees

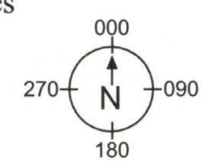

Figure 15. Ground truth examples in the Hill Country west of San Marcos. See text for descriptions. Compass rose is for use with (a) and (b).

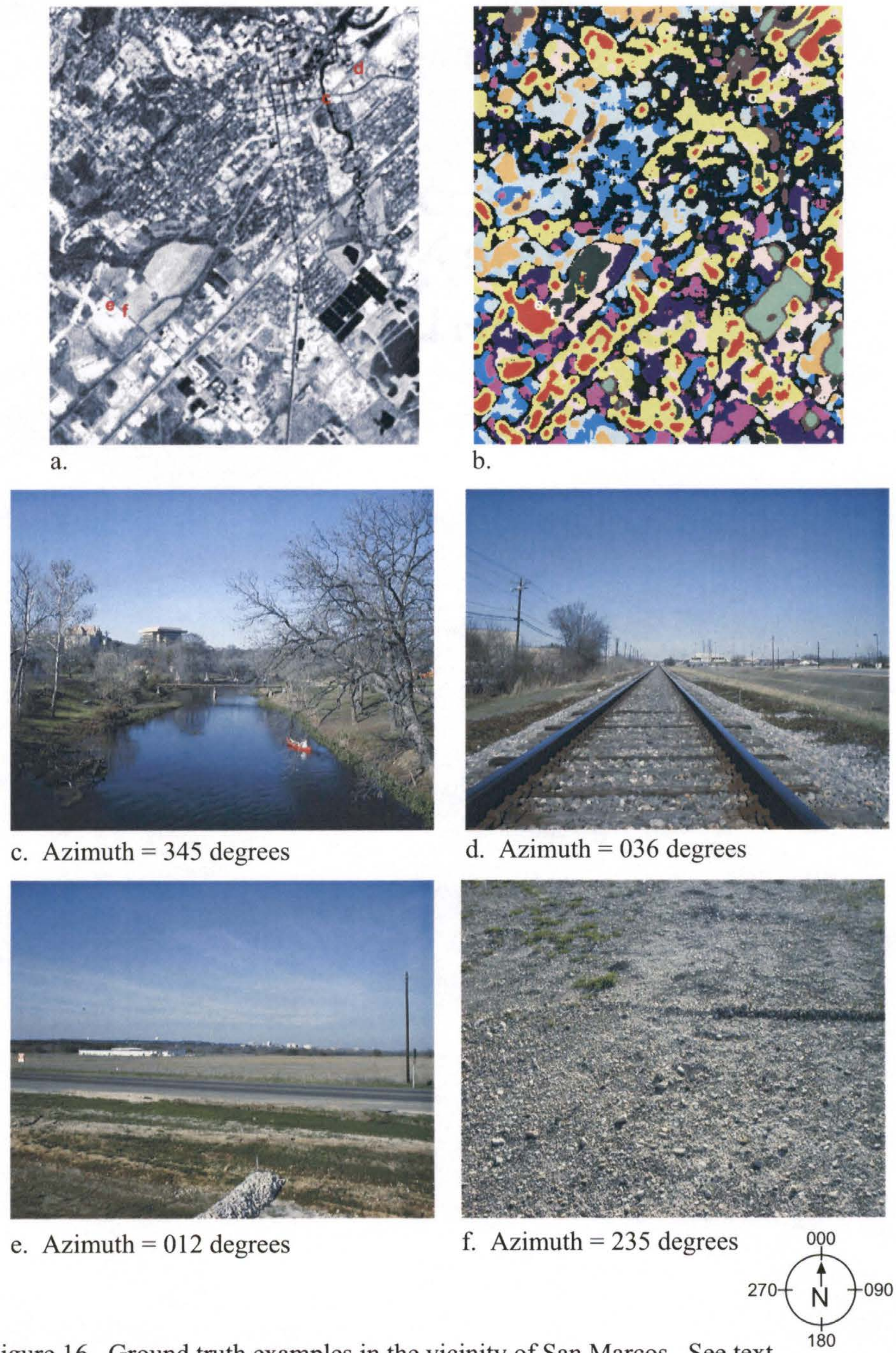

Figure 16. Ground truth examples in the vicinity of San Marcos. See text for descriptions. Compass rose is for use with (a) and (b).

Figure 14 shows ground-based photography examples in the vicinity of downtown Austin, TX. Refer to the classified image map in Figure 6 and associated legend given in Table 7a for the class assignments. Figure 14c and 14d are illustrative of the chaotic mix of land uses contained within the concentrated areas of the inner city, with small businesses and dwellings overshadowed by the more recent large-scale commercial development projects in and around downtown Austin. The blocky silver structure in the middle ground of Figure 14d is the recently constructed Austin Convention Center. The ground surface in the foreground is a highly reflective gravel parking lot, which along with the overall sparseness of vegetation and the abundant presence of large buildings, contributed to the classification of this area in class 8. Figure 14e shows a more distant view of downtown Austin, with the Interstate-35 corridor in the foreground and a typical older residential neighborhood in the left side of the picture. The presence of vegetation proved to be quite significant in determining the class assignment for any given area. Much of this section of the Interstate corridor is characterized by relatively low-density commercial development, with older residential areas occurring on either side to the east and west. Figure 14f is situated on Congress Street in downtown Austin, two blocks south of the Texas State Capitol Building, which appears in the background. This photo presents an interesting illustration of the shadows cast by the tall buildings in Austin's central business district, which offered something of an explanation for the classification of some segments of the downtown area in class 4, a class normally otherwise characterized by older residential areas with abundant woodland vegetation, which have a relatively dark, heterogeneous signature. Areas of large buildings with lower vertical profiles, such as the commercial and industrial districts in other parts of the city, were not subject to this same phenomenon.

Figure 15 shows examples for an area in the Hill Country west of San Marcos along Ranch Road 12. Refer to Figure 7 and Table 7b for the associated classification map and legend. Figure 15c shows the entrance to the Falcon Wood residential subdivision in the foreground, which is representative of the highly reflective linear areas composed of short grass and pavement that characterized class 7. The background of this photograph shows the dense natural woodlands that were characteristic of classes 5 and 6. The scene in Figure 15d is quite typical of the mixed rangelands and woodlands found throughout the Hill Country, and fell into class 11. Figures 15e and 15f, taken in roughly opposite directions from the same location, are illustrative of a transition area from one land use class to another. The foreground of Figure 15e shows the manicured grass entrance to the San Marcos Baptist Academy. This area fell into class 12 and class 4. At the time of satellite image acquisition, this area was likely to have been much drier than it appears in the photo, explaining the classification of grasses into class 4, which is normally characterized by dry rock and concrete. This same situation appears to have occurred at several other locations throughout the entire San Marcos study area, most notably in the fields just to the north of the loop in the Blanco River (see the right side of Figures 9a and 9d). This phenomenon is likely due to the drier than normal period for the two months prior to satellite imagery acquisition (Figure 2). The campus of the Academy, just to the South and West, fell into classes 4 and 10, as expected for concrete structures and large buildings. Figure 15f provides a particularly interesting example of the importance of considering the time-critical nature of certain phenomena that can be observed in satellite imagery. There is a large segment of land to the east of the academy campus that fell into classes 1 and 8. These classes were normally characterized as deep water or topographic shadow. However, the ground photo shown here does not provide any evidence of such a signature; at first this was the source of some confusion. Upon further investigation, local sources indicated the occurrence of a large grass fire in this area just prior to satellite image acquisition, explaining the dark scar that is visible on the satellite imagery, but which is clearly no longer present in the photo (Figure 15f). The power lines in the photo are associated with the nearby utility substation, which appears in the pan imagery as a bright white square just to the south of the location marker seen in Figure 15a. Another area of medium density natural woodlands is visible in the background of the photo. The proximal mixing of natural areas with areas of human impact is quite characteristic of the intensively developed geography of the Texas Hill Country in Hays County.

Figure 16 shows ground-based photography examples and associated ETM+ pan imagery and classification map in the vicinity of the city of San Marcos. Refer to Figure 7 and Table 7b for the associated classification map and legend. Figure 16c is a view looking north along the channel of the San Marcos River. The channel, much of which fell into class 8, was characterized in the imagery by the dark signature typically associated with water. The trees in the adjoining riparian area are deciduous, and thus had a somewhat lighter tone in the imagery than the evergreen woodlands found elsewhere in the Hill Country. The river itself was not wide enough to be recognized consistently as an independent class by the FBCC process at this data resolution, although with the buffer zone of riparian vegetation, it did show up as a linear feature on the classification map in most places. The photo in Figure 16d is located near the San Marcos Public Library along one of the several mainline railroad corridors running through the city. In the distance is Bobcat Stadium, on the right side of the tracks. On the left side and in the middle ground of the photo is Strahan Coliseum. These two structures, along with portions of their associated concrete parking lots, fell into classes 4 and 10, which were typical of large buildings and dry concrete. The railroad corridor itself, unlike the river in Figure 16c, did not show up at all in the FBCC map, although the impression of the linear form of the corridor was evident in some places in the shapes of the areas by which it was bounded. Corridors such as this frequently act as boundaries between adjacent areas of differing land use. The large grassy areas adjacent to the tracks near the San Marcos Public Library (not visible in the photo) fell into class 12.

Figure 16e shows an example of a sizable area of open land vegetated by short grass. This area was classified mainly in classes 12 and 9. In the background lie the eastern edge of the Balcones Escarpment and the elevated buildings of the campus of Southwest Texas State University. In the middle ground to the left is a large, flat building that appeared as a bright square in the pan imagery and as a square of class 10 bounded by class 4 in the FBCC map. The photo in Figure 16f is a low oblique shot of the disturbed ground at a large residential construction site. The ground surface here was composed of fully exposed, very dry, gravelly limestone soil, with a very sparse growth of grass. The extremely high albedo of this surface was typical of the ground cover types that fell into class 10. The relationship of class 10 and class 4 within this part of the study area shows a clear example of the aforementioned boundary effect that was characteristic of the FBCC technique.

Class Merging Example

Figure 17 is given as an example of the class merging procedure, whereby the boundary effect can be minimized. This map is based upon the panchromatic FBCC classification of the San Marcos subset (Figure 7), in which 12 natural groups were classified. Class merging was done in such a way that each "boundary" class was merged with its obvious corresponding class. The value of the technique as it is demonstrated here is that the classification map is simplified. This can be quite useful in cases with a very pronounced boundary effect; in such cases it may be appropriate to merge classes prior to the legend development stage of the classification. This map is provided here only as a simple demonstration of the final product of the FBCC technique. For a more rigorous treatment of the boundary effect and a more stringent method of merging FBCC classes, refer to Eyton (1993).

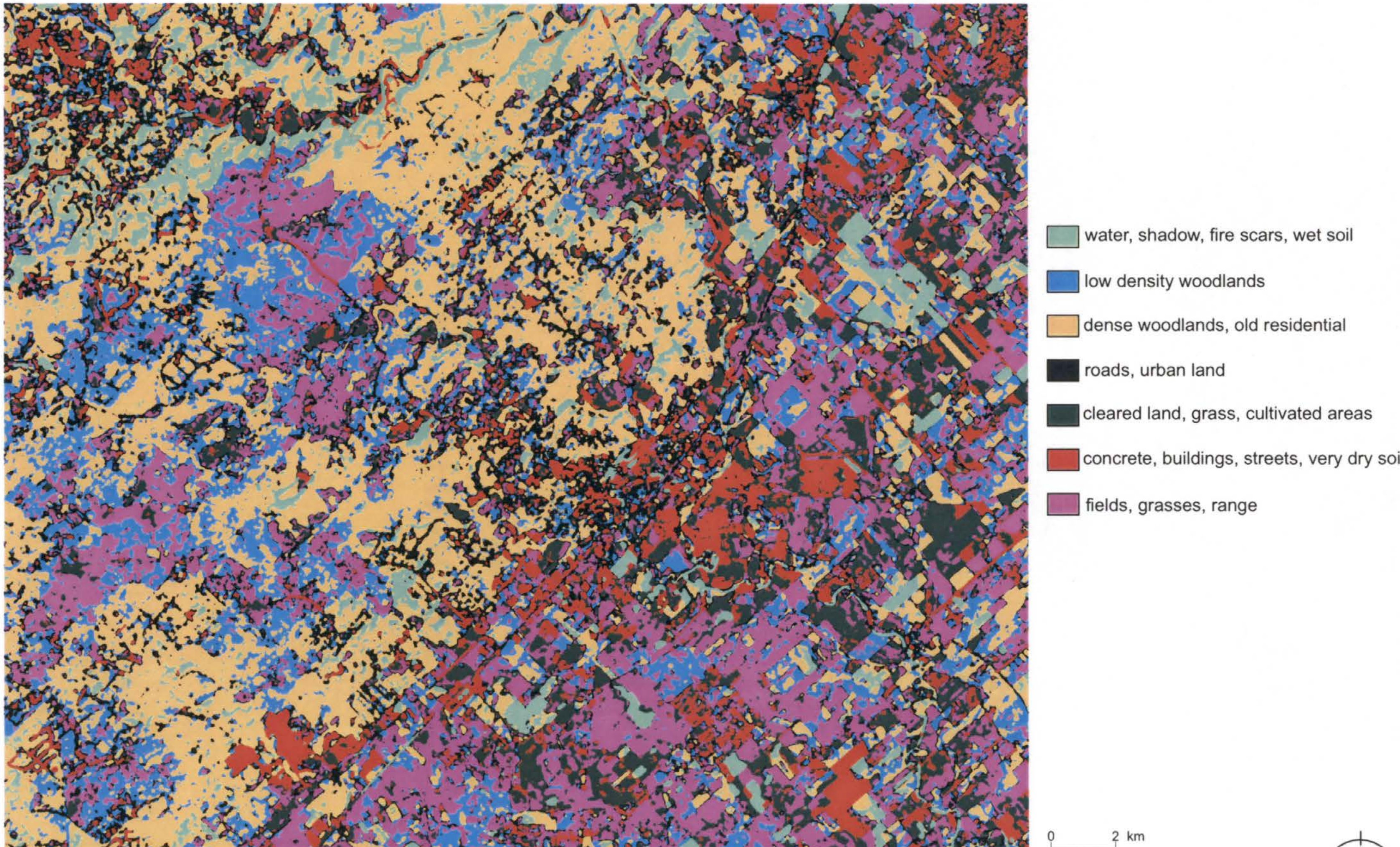

Figure 17. Panchromatic FBCC image map with post-classification merging of classes, San Marcos subset.

CHAPTER VI

SUMMARY, CONCLUSIONS, AND FUTURE WORK

The panchromatic image classification technique explored in this paper serves to highlight the general usefulness of frequency-based contextual classification as an alternative to traditional per-pixel classification. By extracting and classifying information on pixel context, this technique has proven to be a viable method of evaluating the complex adjacency information that exists in digital remote sensing data. This technique especially allows improvements in the classification of urban and suburban areas, an application for which the traditional methods are not well suited. With the increased availability and usage in the civilian and scientific sectors of digital remote sensing data from airborne and space-borne platforms, applications of automated contextual pattern recognition will surely become more widespread.

This study was successful in revealing some distinctive considerations and issues relating to the FBCC processing of panchromatic imagery. Foremost among these are:

1. The FBCC processing of panchromatic imagery using unsupervised training sample selection is a viable and useful method for extracting thematic information content from the imagery, especially if conventional multispectral classification is not an option due to limited availability of data or of resources for data acquisition.

2. The kernel size to be used in FBCC processing must be determined on a case-by case basis, based primarily upon the resolution of the source imagery, the desired unit of analysis for the extraction of context information, and the appropriate level of generalization for the types of land cover or land uses to be analyzed (e.g. urban land use mapping, vegetation mapping, or other applications).
3. The development of a legend for the classified image map resulting from FBCC processing (unsupervised training sample selection) can be partially accomplished by systematic interpretation of image content within each of the classified areas. This systematic analysis is intrinsically useful to the analyst, even though ground truth and other sources of reference information are necessary for development of a truly comprehensive and accurate map legend.
4. The presence, type, and vigor of vegetation in various portions of an image scene are of primary importance to the outcome of an automated classification derived from the panchromatic imagery acquired by the ETM+ sensor.
5. The patterns which can be extracted from a panchromatic image using the FBCC technique are markedly similar to those that can be extracted from multispectral imagery, with one major difference: regions within the panchromatic scene that have similar or identical reflectance signatures (such as water and topographic shadow) cannot be separated by the automated classifier, while they may be separable using the several reflectance values available in a multidimensional image data set. Close attention must be paid during the interpretation of the results of a panchromatic classification to the specific bandwidth range that is recorded by the sensor.

Possible directions for future study of this subject are plentiful. The classification of panchromatic imagery certainly has application within the realm of historical geography; archived panchromatic aerial photos can be digitized by scanning and then thoroughly analyzed using the aforementioned processing techniques. This presents the possibility of time-series analysis of archival imagery, which can be of much value to historians as well as to geographers or planners wishing to use information about past changes in the modeling of future developments. Time series analysis of remotely sensed data could be applied to complex problems in the biogeography and geomorphology of changing landscapes, in addition to tracking the growth of populated areas. The implementation of a truly multitemporal classification scheme, using registered data sets that are separated temporally rather than spectrally, should also enhance the information yield of the classification process, permitting a more robust interpretation of past and current land uses and land use changes. The FBCC methods outlined in this paper would be applicable to such an analysis.

BIBLIOGRAPHY

Barnsley, M.J., and S.L. Barr. 1996. Inferring Urban Land Use from Satellite Sensor Images Using Kernel-Based Spatial Reclassification. *Photogrammetric Engineering and Remote Sensing* 62, no. 8: 949-958.

Charbonneau, L., D. Morin, and A. Royer. 1993. Analysis of Different Methods for Monitoring the Urbanization Process. *Geocarto International* 8, no. 1: 17-25.

Eyton, J.R. 1993. Urban Land Use Classification and Modelling Using Cover-Type Frequencies. *Applied Geography* 13: 111-121.

Eyton, J.R. 1999. *Terra Firma.* Unpublished Software Package for Digital Image Processing and Terrain Analysis, Southwest Texas Sate University.

Fisher, R.A. 1936. The Use of Multiple Measures in Taxonomic Problems. *Annals of Eugenics* 7: 179-188.

Forster, B.C. 1980. Urban Residential Ground Cover Using Landsat Data. *Photogrammetric Engineering and Remote Sensing* 46, no. 4: 547-558.

Fuller, R.M., G.B. Groom, and A.R. Jones. 1994. The Land Cover Map of Great Britain: An Automated Classification of Landsat Thematic Mapper Data. *Photogrammetric Engineering and Remote Sensing* 60, no. 5: 553-562.

Gong, P. and P.J. Howarth. 1990. The Use of Structural Information for Improving Land-Cover Classification Accuracies at the Rural-Urban Fringe. *Photogrammetric Engineering and Remote Sensing* 56, no. 1: 67-73.

Gong, P. and P.J. Howarth. 1992. Frequency-Based Contextual Classification and Gray-Level Vector Reduction for Land-Use Identification. *Photogrammetric Engineering and Remote Sensing* 58, no. 4: 423-437.

Haralick, R.M. and K.S. Sharmugan. 1974. Combined Spectral and Spatial Processing of ERTS Imagery Data. *Remote Sensing of Environment* 3: 3-13.

Hsu, S. 1978. Texture-Tone Analysis for Automated Land-Use Mapping. *Photogrammetric Engineering and Remote Sensing* 44: 1393-1404.

Howard, T. 1998. Frequency-Based Contextual Classification of Land Cover Assemblies from Digital Orthophoto Quarter Quadrangles. Unpublished Directed Research for Master's Degree, Department of Geography and Planning, Southwest Texas State University, San Marcos, TX.

Jackson, M.J., P. Carter, T.F. Smith, and W.G. Gardner. 1980. Urban Land Mapping from Remotely Sensed Data. *Photogrammetric Engineering and Remote Sensing* 46, no. 8: 1041-1050.

Jensen, J.R. 1979. Spectral and Textural Features to Classify Elusive Land Cover at the Urban Fringe. *Professional Geographer* 31, no. 4: 400-409.

Jensen, J.R. 1981. Urban Change Detection Mapping Using Landsat Digital Data. *The American Cartographer* 8, no. 2: 127-147.

Jensen, J.R. 1996. *Introductory Digital Image Processing: A Remote Sensing Perspective*, 2nd ed. Englewood Cliffs, NJ: Prentice Hall, Inc.

Jensen, J.R. and D.L. Toll. 1982. Detecting Residential Land-Use Development at the Urban Fringe. Photogrammetric Engineering and Remote Sensing 48, no. 4: 629-643.

Lillesand, T.M. and R.W. Kiefer. 1994. *Remote Sensing and Image Interpretation*, 3rd ed. New York: John Wiley and Sons.

Moller-Jensen, L. 1990. Knowledge-Based Classification of an Urban Area Using Texture and Context Information in Lansat-TM Imagery. *Photogrammetric Engineering and Remote Sensing* 56, no.6: 899-904.

National Oceanic and Atmospheric Administration (NOAA). 1999. *Climatological Data Annual Summary: Texas,* Vol. 103 (1998) and 104 (1999). Asheville, NC: National Climatic Data Center.

Ramos, M.G., ed. 1997. *1998-1999 Texas Almanac*. Dallas, TX: The Dallas Morning News, Inc.

Richards, J.A. 1993. *Remote Sensing Digital Image Analysis: An Introduction*, 2nd ed. New York: Springer Verlag.

Scarpace, F.L. and B.K. Quirk. 1980. Land Cover Classification Using Digital Processing of Aerial Imagery. *Photogrammetric Engineering and Remote Sensing* 46, no. 8: 1059-1065.

Sharma, K.M.S. and A. Sarkar. 1998. A Modified Contextual Classification Technique for Remote Sensing Data. *Photogrammetric Engineering and Remote Sensing* 64, no. 4: 273-280.

Slocum, T. 1999. *Thematic Cartography and Visualization.* Upper Saddle River, NJ: Prentice-Hall, Inc.

Strahler, A.N. and A.H. Strahler. 1978. *Modern Physical Geography.* New York: John Wiley & Sons, Inc.

Swain, P.H. and S.M. Davis, eds. 1978. *Remote Sensing: The Quantitative Approach.* New York: McGraw-Hill, Inc.

Swanson, E.R. 1995. *Geo-Texas: A Guide to the Earth Sciences.* College Station, TX: Texas A&M University Press.

Texas Natural Resources Information System. 1999. Landsat 7 ETM+ Digital Data, Scene ID#LE7027039009926150, Path 27, Row 39, September 18, 1999.

Toll, D.L. 1984. An Evaluation of Simulated Thematic Mapper Data and Landsat MSS Data for Discriminating Suburban and Regional Land Use and Land Cover. *Photogrammetric Engineering and Remote Sensing* 50, no. 12: 1713-1724.

Wharton, S.W. 1982a. A Context-Based Land-Use Classification Algorithm for High-Resolution Remotely Sensed Data. *Journal of Applied Photographic Engineering* 8, no. 1: 46-50.

Wharton, S.W. 1982b. A Contextual Classification Method for Recognizing Land Use Patterns in High Resolution Remotely Sensed Data. *Pattern Recognition* 15, no. 4: 317-324.

Wood, R.A., ed. 1996. *Weather of U.S. Cities,* 5th ed. Detroit, MI: Gale Research Co.

VITA

Matthew Edward Ramspott was born in West Point, Nebraska, on August 30, 1972, the son of Edward Lee Ramspott and Pamela Rose (Kaup) Ramspott. Upon completing work at Blair High School, Blair Nebraska, he enrolled in 1990 at the University of Nebraska-Lincoln (UNL) as a Regent's Scholar. He received the degree of Bachelor of Science in 1995, with a major in Environmental Studies. While earning his undergraduate degree, he was employed as a research assistant in the Department of Biological Sciences at UNL. From 1995 through 1997, he was employed variously in the fields of environmental education and research, field archaeology, medical insurance marketing research, and framing carpentry. During the summer of 1997 he attended the National Outdoor Leadership School, Lander, Wyoming, completing a course in natural history and wilderness survival. From the fall of 1997 to spring of 1998, he attended Oregon State University, Corvallis, Oregon, as a post-baccalaureate student, taking courses in physical geography, GIS, and cartography. During the summer of 1998, he worked as a land surveyor's assistant at Kirkham Michael Engineering Consultants, Omaha, Nebraska. In August of 1998, he entered the Master of Applied Geography program at Southwest Texas State University (SWT), San Marcos, Texas. During his time at SWT, he was co-author of a publication entitled *The Use of Remote Sensing in Detecting and Analyzing Natural Hazards and Disasters, 1972-1998: A Partially Annotated Bibliography*. He was the winner of several awards including: Honorable Mention in the 1999 cartography competition of the National Geographic Society; 2nd Prize in the student poster competition of the 1999 meeting of the Southwest Division, Association of American Geographers; the 2000 John Wiley Award for Excellence in Geography (administered by the SWT Geography Department); and the Madison and Lila Self Ph.D. Fellowship at the University of Kansas. He has been a member of the Phi Beta Kappa academic honor society since 1995 and a student member of the American Society for Photogrammetry and Remote Sensing since 1998.

Permanent address: P.O. Box 78
Blair, Nebraska 68008

This thesis was typed by Matthew Edward Ramspott